DOI: 10.1590/2317-4889201720170019

ARTICLE

Post-collisional basalts of the Acampamento Velho Formation, Camaquã Basin, São Gabriel Terrane, southernmost Brazil

Basaltos pós-colisionais da Formação Acampamento Velho, Bacia do Camaquã, Terreno São Gabriel, sul do Brasil

Luiz Alberto Vedana[1]*, Ruy Paulo Philipp[2], Carlos Augusto Sommer[3]

ABSTRACT: The basic volcanic rocks in the Palma region, southern portion of the São Gabriel Terrane, have always been interpreted as generated during the active subduction period of the São Gabriel orogeny (Cryogenian). This terrane was built as the result of the Charrua Ocean closure between 900–680 Ma. The basalts show a subhorizontal igneous flow foliation and porphyritic texture, with plagioclase phenocrysts in a thin matrix composed of plagioclase, augite and magnetite, commonly altered to actinolite, chlorite and epidote. They have amygdales and veinlets reflecting a pervasive hydrothermal phase and are affected by thermal metamorphism related to Jaguari granite intrusion. Two samples were dated by the U-Pb zircon geochronology and yielded crystallization ages of 563±2 Ma and 573±6 Ma. The basalts have transitional composition from tholeiitic to calc-alkaline, metaluminous character, trace elements patterns rich in large-ion lithophile element (LILE) with negative anomalies of Nb, P and Ti, slight enrichment in light rare-earth elements (LREE) and horizontal pattern of heavy rare earth elements (HREE). The data allow interpreting the basalts as belonging to the Acampamento Velho Formation of the Camaquã Basin, and related to the basalts of the Ramada and Taquarembó plateaus. These associations represent the final evolution of the volcanism generated in the post-collisional period of the Dom Feliciano Belt.

KEYWORDS: Dom Feliciano Belt; São Gabriel Terrane; Camaquã Basin; Acampamento Velho Formation; Basalt; Ediacaran.

RESUMO: *As rochas vulcânicas básicas da região da Palma, porção sul do Terreno São Gabriel, foram interpretadas como se tivessem sido geradas durante o período de subducção ativa da orogenia São Gabriel (Criogeniano). Esse terreno formou-se como resultado do fechamento do Oceano Charrua, entre 900–680 Ma. Os basaltos possuem foliação ígnea sub-horizontal e textura porfirítica, com fenocristais de plagioclásio em matriz fina compostos de plagioclásio, augita e magnetita, a qual é comumente alterada para actinolita, clorita e epidoto. As rochas apresentam amígdalas e venulações refletindo uma fase hidrotermal pervasiva e são afetadas por metamorfismo termal relacionado à intrusão do granito Jaguari. Duas amostras foram datadas pelo método geocronológico U-Pb em zircão e revelaram idades de cristalização de 563±2 Ma e 573±6 Ma. Os basaltos possuem composição transicional toleítica a calcioalcalina, característica metaluminosa, padrão de elementos traços enriquecidos em elementos litófilos de raio iônico grande (LILE) com anomalias negativas de Nb, P e Ti, leve enriquecimento em elementos terras raras pesados (LREE) e padrão horizontal de elementos terras raras leves (HREE). Os dados permitem interpretar os basaltos como pertencentes à Formação Acampamento Velho da Bacia do Camaquã e relacionados aos basaltos dos platôs Ramada e Taquarembó. Essas associações representam a evolução final do vulcanismo gerado no período pós-colisional do Cinturão Dom Feliciano.*

PALAVRAS-CHAVE: *Cinturão Dom Feliciano; Terreno São Gabriel; Bacia do Camaquã; Formação Acampamento Velho; Basaltos; Ediacarano.*

[1]Professor of the Faculty of Engineering, Centro Universitário Ritter dos Reis – UniRitter, Porto Alegre (RS), Brazil. *E-mail: luizvedana@gmail.com*

[2]Professor of the Departamento de Mineralogia e Petrologia (DEMIPE), Universidade Federal do Rio Grande do Sul – UFRGS, Porto Alegre (RS), Brazil. *E-mails: ruy.philipp@ufrgs.br, casommer@sinos.net*

[3]Professor of the Department of Geodesy – UFRGS, Porto Alegre (RS), Brazil. *E-mail: casommer@sinos.net*

*Corresponding author.

Manuscript ID: 20170019. **Received in:** 13/02/2017. **Approved in:** 07/18/2017.

INTRODUCTION

Recognizing the composition and meaning of the volcanic rocks is important in the characterization of sedimentary basins and oceanic crust subduction processes. The difficulties in rock classification are associated to the low degree of crystallinity of the matrix, whose characterization depends on obtaining their chemical composition. Similarly, the presence of volcanic rocks is associated with the occurrence of partial crust and/or mantle melting processes, and with the existence of structures such as faults, that allow the rise and outpouring of lava. The chemical composition of the volcanic rocks is essential to characterize the magmatic series and to assess the fractionation processes, the occurrence of assimilation and the sources of magmas. These factors, associated with the regional geology and geochronology features, define their tectonic significance.

The Brasiliano Orogeny Cycle in Rio Grande do Sul is represented by the Dom Feliciano Belt (DFB), which is a unit consisting of rock associations developed during three orogenic events. These orogenies were called Passinho (900–860 Ma), São Gabriel (770–680 Ma) and Dom Feliciano (650–540 Ma), and are characterized by a wide generation of igneous, metamorphic and sedimentary rocks (Chemale Jr. 2000, Hartmann *et al.* 2007, Saalmann *et al.* 2010, Philipp *et al.* 2016). The units that represent the subduction period and juvenile accretion are restricted to the São Gabriel Terrane (SGT). This terrane is the western portion of the DFB and features an elongated shape in the N20-30ºE direction, about 110 km long and 60 km wide (Fig. 1). The composition of the SGT is defined by the tectonic intercalation of ophiolite complexes with metavolcano-sedimentary associations and granite-gneiss complexes (Fig. 2). This interleaving is characterized by the thrusting of elongated bodies in the NE-SW direction, through ductile shear zones of medium angle and eastward vergence.

The Palma Complex was proposed by Garcia and Hartmann (1981) to designate a flysch-type sequence arranged as an elongated structure, in the N30ºE direction, exposed between São Gabriel and Lavras do Sul (RS) regions, extending from 5 km, south of Palma village, up to about 20 km, northeast of it. The complex is subdivided into two major associations composed of metasedimentary and meta-igneous rocks (granites, metadacites, meta-andesites, metabasalts, metagabbros,

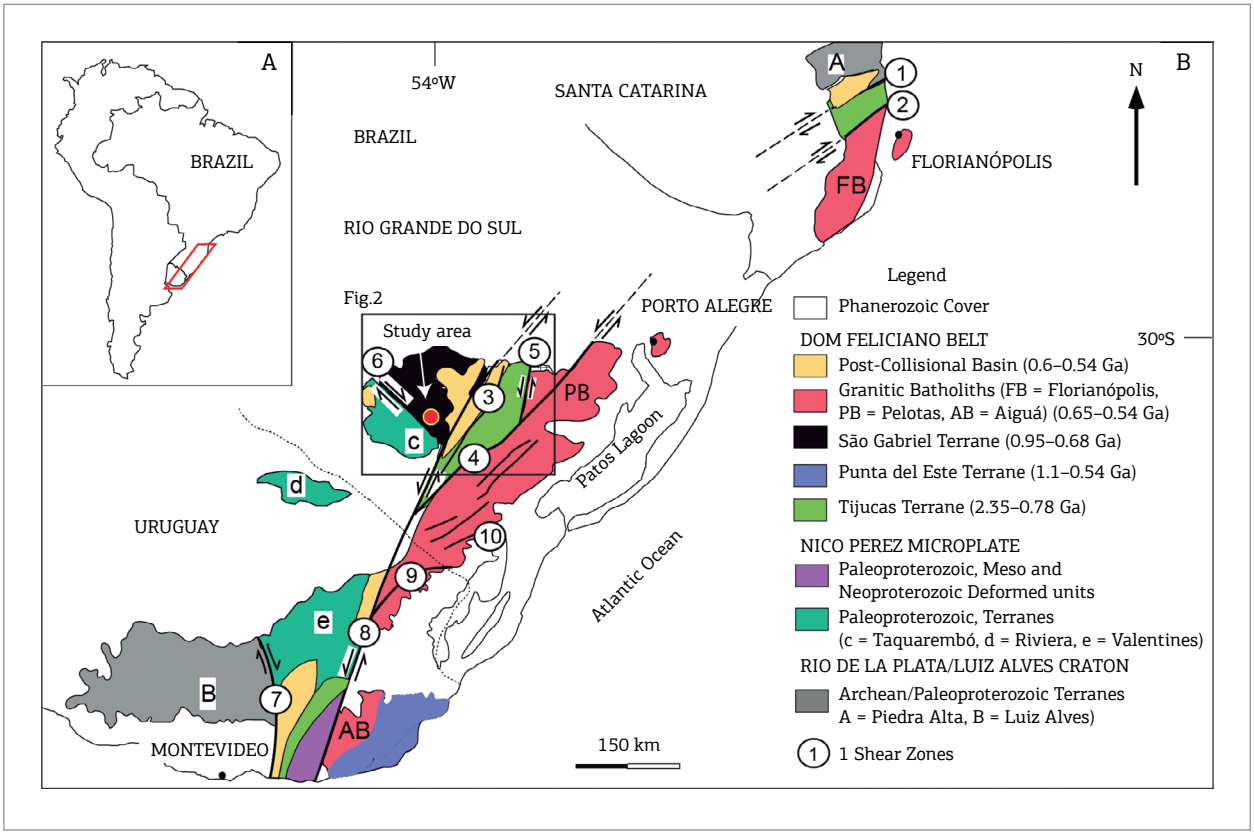

Figure 1. (A) Location of the study area in the context of South America. (B) Geologic map of the southern Brazilian and Uruguay shields, map and data compiled by Philipp et al. (2016). Shear zones: (1) Itajaí-Perimbó; (2) Major Gercino; (3) Santana da Boa Vista; (4) Dorsal de Canguçu; (5) Passo do Marinheiro; (6) Ibaré; (7) Sarandi del Yí; (8) Sierra Ballena; (9) Cerro Amaro; (10) Arroio Grande.

meta-ultrabasic rock and lamprophyres). Other authors have adopted similar proposals, recognizing these groups of rocks and associating them to subduction processes and orogenic regional metamorphism (Chemale Jr. 1982, Santos *et al.* 1990, UFRGS 1996, Laux *et al.* 2012).

This article proposes the separation of the unit originally characterized as metavolcanic in this context, since the obtained petrological and geochronological data associate this unit to volcanism of a more recent age, correlated to the Acampamento Velho Formation, Camaquã Basin (CB).

The main goal of this article was to characterize the mafic volcanic rocks occurring in the Palma region, through the stratigraphic relationships obtained with field data, combined with petrographic, geochemical and geochronological data. The described basalts were compared with other mafic volcanic rocks belonging to the Acampamento Velho Formation, 20 km to the northeast, on the Ramada Plateau, and about 20 km to the southeast, on the Taquarembó Plateau.

MATERIALS AND METHODS

This survey was based on the integration of the contact relationships obtained in geological mapping in 1:25.000 scale with structural, petrographic and geochemical data. Ten samples of mafic volcanic rocks were analyzed, with U-Pb zircon geochronological analyses of two basalt samples.

The thin sections were prepared in the Institute of Geosciences of Universidade Federal do Rio Grande do Sul (UFRGS). The steps of sample preparation are:

- Cutting a slab: a slide is cut from a piece of rock collected in field;
- Initial lapping on the slab: on side of the sample is lapped flat and smooth on a cast iron lap with 400 and 600 grit carborundum;
- Glass slide: glass slide is glue with epoxy on the lapped face of the slab;
- Section: using a saw, the slab is cut-off for reduce the thickness;
- Final lapping: using a hand on a glass plate the thickness of 30 microns are achieved with 600 grit carborundum;
- Polishing: the polishing is made with a spun on a polishing machine using nylon and diamond paste.

The geochemical analyses were obtained at Acme Laboratories LTDA. by Inductively Coupled Plasma (ICP), for the major elements with detection limit of 0.01% and for V, Ba, Sr, Y and Zr, with a detection limit of 1 to 5 ppm. The analyses of trace elements and rare earth elements were obtained by Inductive Coupled Plasma – Mass Spectrometry

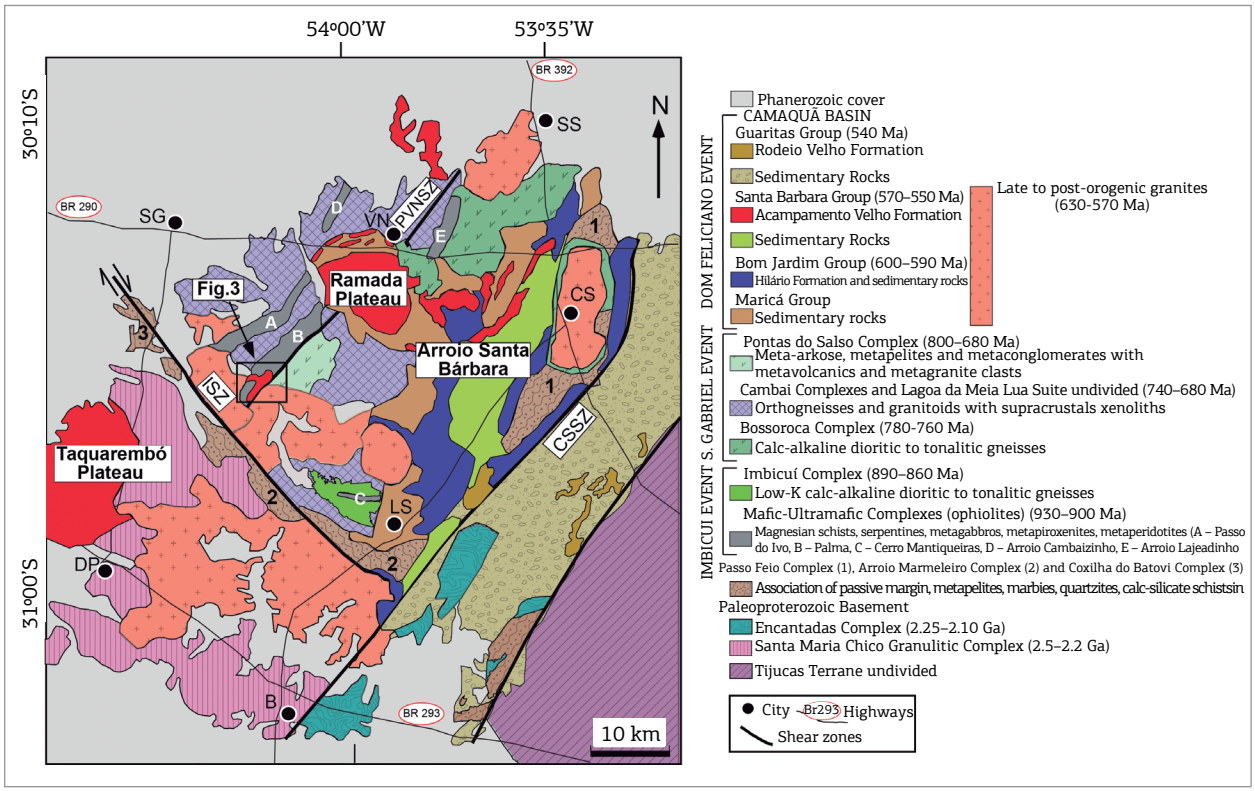

Figure 2. Geological map of the São Gabriel Terrane. Cities: SS –- São Sepé; CS – Caçapava do Sul; VN – Vila Nova do Sul; LS – Lavras do Sul; DP – Dom Pedrito; B – Bagé. Shear zones: SZPVN – Shear Zone Passinho/Vila Nova; SZI – Shear Zone Ibaré; SZCS – Shear Zone Caçapava do Sul; DEF – Dom Feliciano Event. Modified from Philipp et al. (2016).

(ICP-MS), with detection limit of 0.005 to 2 ppm. The analytical protocol at the ACME Laboratories included the analysis of Standard SO-18 and Blank (STD SO-18 and BLK) and of four sample duplicates. The samples were milled in an agate mill. Representative samples were selected and were not affected by weathering.

In order to carry out Laser Ablation-Multi Collector-Inductively Coupled Plasma Mass Spectrometry (LA-ICP-MS) U-Pb zircon analysis, two samples of basalts of the Arroio da Palma stream (LV-53 and LV-70) were crushed and milled using a jaw crusher, and then reduced to powder in a disk mill.

Zircon grains were concentrated by conventional magnetic and heavy liquid procedures, the final concentration was carried out by hand picking. To avoid bias introduced during handpicking, no visual morphological or color differentiation was made. These steps were made at UFRGS at the sample preparation laboratories.

The grains used for zircon dating were mounted in epoxy resin, polished using diamond paste to expose their inner parts. Imaging was made by backscattered electrons (BSE) and cathodoluminescence (CL) to determine their internal structures and crystallization phases. Only zircon grains free of imperfections, fractures, and mineral inclusions were selected for isotopic analysis. The most clear and inclusion-free minerals were selected for LA-ICP-MS analyses. CL images of zircon were obtained using a Quanta 250 FEG electron microscope equipped with Mono CL3+ CL spectroscope (Centaurus) at the Geochronological Research Center in Universidade de São Paulo (USP), Brazil.

Isotopic data were obtained using a NEPTUNE ICP-MS coupled with an excimer laser ablation system. The cup configurations optimized for U-Pb data acquisition were IC3 = ^{202}Hg, IC4 = ^{204}(Hg+Pb), L4 = ^{206}Pb, IC6 = ^{207}Pb, L3 = ^{208}Pb, H2 = ^{232}Th and H4 = ^{238}U, in which L and H were low, with a high mass to faraday cup position, and ICs are ion counting (continuous dynode system). The ICP configurations were: radio frequency power = 1,100 W; cool gas flow rate = 15 L/min (Ar); auxiliary gas flow rate = 0.7 L/min (Ar); sample gas flow rate = 0.6 L/min. Laser Setup: energy = 6 mJ, repetition rate = 5 Hz, spot size = 25–38 µm, helium carrier gas = 0.35 + 0.5 L/min. The routine U-Pb analysis consists of two blanks, two National Institute of Standards (NIST), three external standard (GJ1 standard), 13 unknown samples, two external standards and two blank measurements. Each run consisted of 40 cycles, with 1 second per cycle. The ^{204}Hg interference on ^{204}Pb was corrected by ^{202}Hg, and the value of ^{204}Hg/^{202}Hg ratio is 4.2. ^{207}Pb/^{206}Pb ratio normalization was achieved by combined NIST and external standards. ^{206}Pb/^{238}U ratio normalization was achieved by external standards. The GJ1 standard (602±4.4 Ma, Elhlou *et al.* 2006) was used for mass bias correction. Zircon typically contains low concentrations of common Pb. Thus, the reliability of the measured ^{207}Pb/^{206}Pb and ^{206}Pb/^{238}U ratios is critically dependent on accurate assessment of the common Pb component. The residual common Pb was corrected according to the measured ^{204}Pb concentration using the known terrestrial composition (Stacey and Kramer 1975).

The uncertainty introduced by laser-induced fractionation of elements and mass instrumental discrimination were corrected using a reference standard of zircon (GJ-1) (Jackson *et al.* 2004). The isotope ratios and inter-element fractionation of data obtained by the ICP-MS were evaluated by interspersing the GJ-1 zircon standard in every set of 13 zircon samples (spots). The GJ-1 standard meets the requirements for the methods used in our laboratory, and the ratios of ^{206}Pb*/^{238}U, ^{207}Pb*/^{206}Pb* and ^{232}Th/^{238}U were homogeneous throughout the application of bracket technique. External errors were calculated using error propagation of the individual measurements of the standard GJ-1 and measurements of the individual zircon samples (spots). Age calculation was made using Isoplot version 4 based mainly on ^{206}Pb/^{238}U (Ludwig 2008). Chemale Jr. *et al.* (2012) detailed the analytical methods and data treatment.

GEOTECTONIC CONTEXT

The Dom Feliciano Belt and São Gabriel Terrane

The Sul-Rio-Grandense Shield comprises Paleo and Neoproterozoic tectonostratigraphic units, including fragments of the Rio de La Plata and Luiz Alves cratons (Chemale Jr. 2000, Hartmann *et al.* 2007, Saalmann *et al.* 2010, Philipp *et al.* 2016). These fragments are composed of Paleoproterozoic and Mesoproterozoic metamorphic and granitic rocks, surrounded the Dom Feliciano Belt, a Neoproterozoic orogen derived from the collision of the Rio de La Plata and Kalahari cratons (Fernandes *et al.* 1992, Saalmann *et al.* 2010, Philipp *et al.* 2016).

The DFB is divided from west to east as follows:

- São Gabriel Terrane;
- Tijucas Terrane;
- Florianópolis-Pelotas-Cutillo-Dionísio Batholiths;
- Punta del Este Terrane (Fig. 1).

The DFB formed during a long-lived evolution of ca. 450 Ma, with three distinct events may be recognized:

- The development of the Passinho Arc (890–860 Ma);
- The São Gabriel Arc (770–680 Ma);
- The Dom Feliciano Arc (650–550 Ma) (Saalmann *et al.* 2010, Philipp *et al.* 2016).

The units of the SGT represent the subduction period of the Brasiliano orogenesis in the Sul-Rio-Grandense Shield. The units that constitute this terrane have accretionary features and correspond to a juvenile Neoproterozoic crust segment, consisting of the tectonic intercalation of metavolcano-sedimentary associations, paragneisses, orthogneisses and meta-granites, cutting by undeformed granitoids (Babinski *et al.* 1996, Philipp *et al.* 2008, Saalmann *et al.* 2010, Hartmann *et al.* 2011, Lena *et al.* 2014, Gubert *et al.* 2016) (Fig. 2). These units characterize the upper and lower portions of the São Gabriel magmatic arc (Chemale Jr. 2000, Saalmann *et al.* 2005, Hartmann *et al.* 2007) and are also intercalated by metamafic-ultramafic sequences that represent ophiolitic associations.

The Palma Complex

The Palma Complex was proposed by Garcia and Hartmann (1981) as composed by two associations:

1. Metasedimentary rocks represented by quartzites, metapelites, metarkoses, marbles and metamarls, interspersed with metaultramafic and metamafic rocks;
2. Metaigneous rocks represented by granites, metadacites, metandesites, metabasalts, metagabbros, metaultrabasic rocks, and lamprophyres.

The complex was subdivided by Chemale Jr. (1982) recognized the Cerro da Cruz and Pontas do Salso sequences. The first one consisting of metaultramafites, metabasites, metapelites and quartzites, marbles and calc-silicate rocks with restricted interbedding of metarhyolites and metandesites. The second sequence consisted of calc-silicate rocks, pelitic and arkosean metasediments, metamorphosed to amphibolite facies. Santos *et al.* (1990) have redefined the Pontas do Salso Sequence as Pontas do Salso Formation.

More recently, the geological mapping conducted by UFRGS (1996) redefined the Pontas do Salso Group as the Monumento and Arroio da Palma formations. The first one consists of epiclastic metasedimentary rocks, metatuffites, metapelites, metasandstones and metaconglomerates, while the latter is represented by metabasalts, metandesites and metadacites.

In mapping conducted by the Geological Survey of Brazil (Laux *et al.* 2012), the Metamorphic Palma Complex was subdivided into three units:

1. Cerro do Ouro Formation, consisting of serpentinites, magnesian schists, basic schists, amphibolites and metagabbros;
2. Pelitic calc-silicate unit, composed of marbles, quartzites, chlorite schists and BIF's;
3. Metavolcanic unit, consisting of metadacites and metandesites.

Laux *et al.* (2012) interpreted the Palma Complex as an ophiolite complex related to the subduction process that occurred in the Cryogenian period.

The Camaquã Basin

The CB was deposited on the central portion of the Sul-Rio-Grandense Shield, during the tardi- to post-collisional period of the Dom Feliciano Belt covering the igneous and metamorphic units of the Taquarembó, São Gabriel and Tijucas terranes, and over the Pelotas Batholith the three ones included in the belt.

The CB is a depositional locus consisting of four distinct cycles of deposition defined by different sedimentary and volcano-sedimentary units, associated with plutonic igneous rocks, separated from each other by angular or erosive regional unconformities (Chemale Jr. 2000, Paim *et al.* 2000, Almeida *et al.* 2012, Janikian *et al.* 2012).

These cycles have been identified in the lithostratigraphy as Maricá, Bom Jardim, Santa Bárbara and Guaritas groups (Gõni *et al.* 1962, Robertson 1966, Ribeiro *et al.* 1966, Ribeiro and Fantinel 1978, Chemale Jr. & Babinski 1995, Paim *et al.* 2000, Almeida *et al.* 2009, 2010, Janikian *et al.* 2012). The proposed subdivisions were established from angular unconformity relationships, sedimentary facies associations, paleocurrents, volcanic associations and, more recently, with the support of provenance studies by U-Pb detrital zircon ages (Borba *et al.* 2008, Hartmann *et al.* 2008, Bicca *et al.* 2013, Oliveira *et al.* 2014).

The sedimentary and volcanic rocks of the CB have deposition ages between 600 and 540 Ma. The volcanic rocks of the Hilário Formation, Bom Jardim Group, have Ar-Ar and U-Pb SHRIMP and LA-ICP-MS zircon ages between 600 and 590 Ma. The acidic volcanic rocks of the Acampamento Velho Formation, Santa Barbara Group, have two U-Pb zircon age groups, between 580–570 and 550 Ma (Wildner *et al.* 1999, Sommer *et al.* 2005, Almeida *et al.* 2010, Almeida *et al.* 2012, Janikian 2004, Janikian *et al.* 2012, Oliveira *et al.* 2014, Matté *et al.* 2016). The andesites of the Rodeio Velho Formation, Guaritas Group, have U-Pb zircon age around 547±6.5 Ma (Almeida *et al.* 2012).

THE ACAMPAMENTO VELHO FORMATION

The Acampamento Velho Formation is a bimodal volcanic/plutonic association of sodium alkaline affinity, mainly characterized by effusive deposits of basic lavas at the base (basalts, trachybasalts and basalt-andesites), followed by explosive ignimbrite deposits, volcanic breccias, and tuffs that are covered by acidic lavas (trachytes and

rhyolites) at the top (Sommer *et al*. 1999, 2005, Almeida *et al.* 2002, Janikian *et al*. 2012, Matté *et al.* 2016). There are four main occurrences of the Acampamento Velho Formation as follow:

1. Taquarembó Plateau (Taquarembó Terrane);
2. Ramada Plateau;
3. Arroio Santa Bárbara (SGT);
4. Swarm dikes in Piratini and Pinheiro Machado and others regions (Pelotas Batolith).

According to Sommer *et al*. (2011) and Matté *et al*. (2016), there is a predominance of juvenile magmatic components in the pyroclastic deposits, such as crystaloclasts, pumices and glass shards, while lithoclasts are more numerous on the basal portions, and mainly connate. The geometry of the deposits and the degree of welding is variable, from stratified and partially welded deposits, to highly welded massive ignimbrites. With respect to the lavas, the autobrecciated, foliated and massive structures are the most common ones. The authors also stress that the preservation of typical features of primary pyroclastic processes, typical of high temperature flows and large amount of gases, associated with the occurrence of lavas and hypabyssal bodies, indicate subaerial volcanism, possibly related with volcanic calderas.

Petrographic and geochemical studies of the basic rocks in the Palma region were conducted by several authors (Garcia 1980, UFRGS 1996, Strieder *et al.* 2000, Lopes & Hartmann 2003, Laux *et al.* 2012). However, geochronological studies (U-Pb) had not been performed in the area.

RESULTS

Field and petrography descriptions

The basalts of the Acampamento Velho Formation occurring in the Palma region form a continuous body, elongated in the N50–60ºE direction, approximately 10 km long and 5 km wide. Volcanic rocks cover the metasediments of the Pontas do Salso Complex in the NE portion, and the metaultramafites of the Palma Ophiolite, in the SW portion. They show tectonic contacts by transcurrent faults with the metaultramafic rocks and host orthogneisses of the Cambaí Complex in the NW portion of the body, and by normal fault with the Jaguari Granite, in its southernmost portion. The main outcrops are along the Palma stream, where were collected the LV-70 sample, which are in a small body (< 5 m^2) in the right margin of the Vacacaí River (Fig. 3). The contact with metagabbro shown in the map of Fig. 3 was not apparent. Near the Granite Jaguari contact, the basalts are cut by tabular bodies of pink leucocratic aplites with low thickness (< 3 m).

The basalts are grayish green in color and show massive apparent structure, with thin flow lamination in altered terms (Fig. 4A and 4B). The average foliation orientation is N40ºE, with soft NW dipping. The main texture is porphyritic, characterized by low concentrations of plagioclase phenocrysts, 1 to 5 mm in size, immersed into a fine equigranular to aphanitic matrix composed of clinopyroxene, plagioclase and magnetite (Fig. 4C and 4D). The top portions feature a large amount of ellipsoidal-shaped amygdales and vesicles, with sizes between 5 and 15 cm. They are filled by quartz, epidote, chlorite, zeolite and carbonate (Fig. 4E and 4F).

They feature three patterns of rectilinear and subvertical fractures, oriented in the NW-SE, NE-SW and E-W directions. The fractures are rectilinear, with spacing between 10 and 40 cm, and often filled with veins of quartz and carbonate, accompanied by the disseminated occurrence of pyrite, chalcopyrite and magnetite.

Under the microscope, the flow foliation is defined by the alignment of plagioclase phenocrysts. The porphyritic texture is characterized by with up to 15% of plagioclase phenocrysts of elongated euhedral prismatic shape, highly sericitized, surrounded by very fine to fine equigranular matrix composed of clinopyroxene and plagioclase, with magnetite, titanite and apatite and opaque minerals as accessories. The matrix is commonly transformed by hydrothermalism and thermal metamorphism, with intense replacement of clinopyroxene by actinolite, chlorite and epidote, and of the plagioclase by aggregates of sericite and epidote, with variable occurrence of carbonate (Fig. 4D). Actinolite has elongated prismatic shape and acicular habit, forming disoriented porphyroblasts of up to 1 mm in size. These transformations are recorded throughout the length of the body of mafic volcanic rocks.

Geochemistry

The obtained geochemical analyses (Tab. 1) added the analyses of Lopes and Hartmann (2003) were compared with the available analyses of basalts and andesites of the Acampamento Velho Formation outcropping in the Taquarembó (Wildner *et al.* 2002) and the Ramada plateaus (Sommer *et al.* 2005, Matté *et al.* 2016).

The mafic volcanic rocks of the Palma region feature subalkaline affinity and are classified as basalts and andesitic basalts (Fig. 5A). The ratios between alumina and alkalis define a metaluminous character (Fig. 5B). In AFM (Irvine & Baragar 1971) and FeOt/MgO vs. SiO_2 diagrams

(Miyashiro 1974), the samples are arranged on the boundary between the fields of calc-alkaline and tholeiitic rocks (Fig. 5C and 5D). The calc-alkaline composition is reinforced in the Jensen diagram (1976) and characterized as a medium-K type (Le Maitre *et al.* 1989) (Fig. 5E and 5F). The subalkaline character is also seen in trace elements, as seen in the Winchester and Floyd (1977) diagrams (Fig. 6A and 6B).

The correlation between the composition of trace elements and rare earth elements of the Palma region mafic volcanic rocks, with similar occurrences found in the Acampamento Velho Formation in the Taquarembó and Ramada plateaus, was conducted in multi-element diagrams (spidergrams) normalized to primitive-mantle values. The three sets of samples show a similar pattern, characterized by slight enrichment in Rb, Ba and Th, negative Nb, P and Ti anomalies, and horizontal heavy rare earth elements (HREE) pattern. This affinity is even more evident with the basic low-Ti type rocks of both plateaus based in

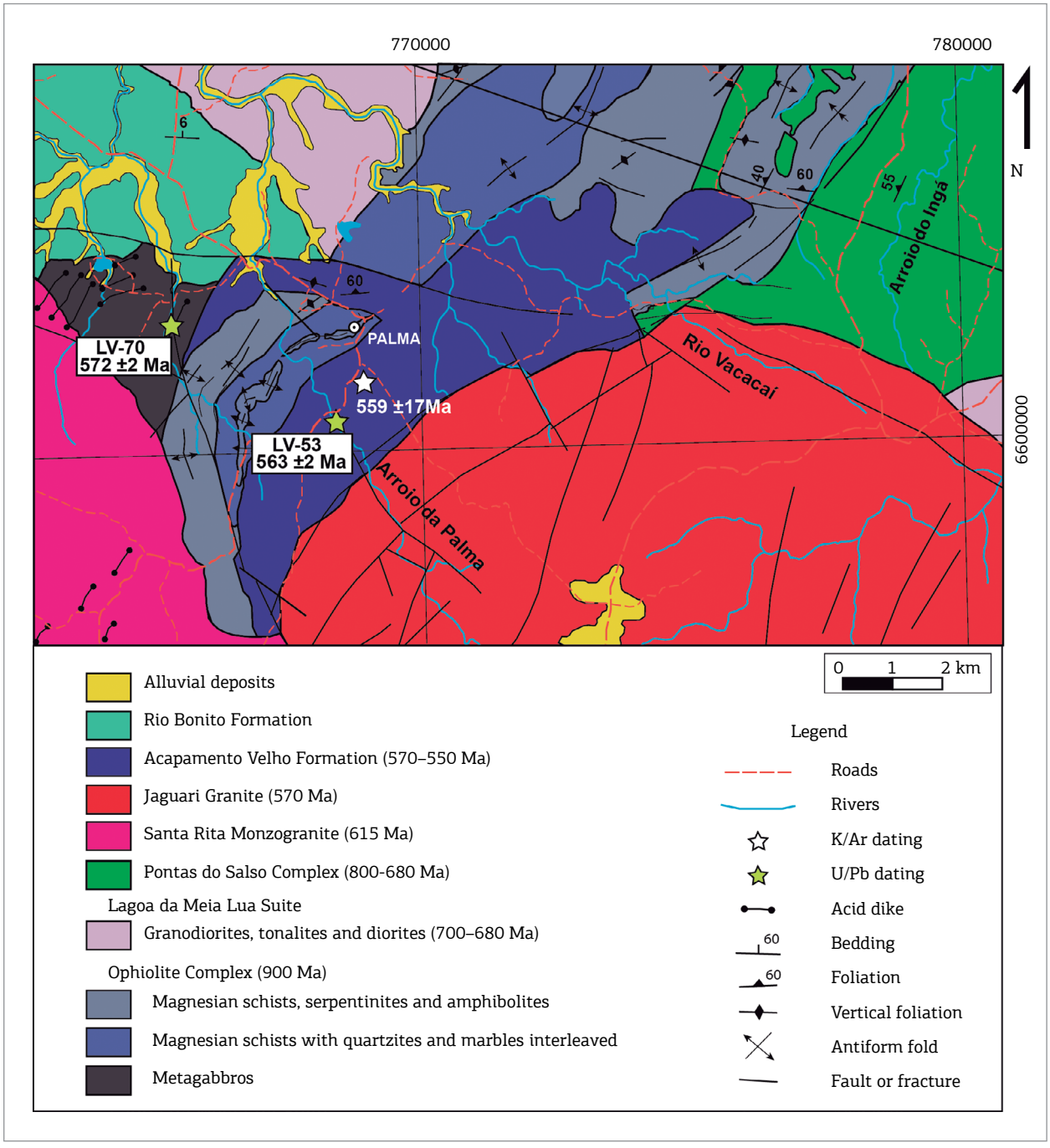

Figure 3. Geological map of the Palma region, central portion of the São Gabriel Terrane. Modified from Laux *et al.* (2012).

the works by Wildner *et al.* (2002), Sommer *et al.* (2005) and Matté *et al.* (2016). High-Ti and low-Ti are evolutionary trends and vary with the SiO_2 content. In the case of basalts, above 2.0% of TiO_2 will be high-Ti, and below, low-Ti. Considering the intermediate and acidic values will be less than 2.0%. However, the general contents of elements are lower for the Palma basalts, which have a very similar composition with the medium-K calc-alkaline basalts of the Honshu arc, in Japan, and different from the high-K basalts of Stromboli volcano (Fig. 7A and 7B). The mafic rocks feature similar chondrite-normalized rare earth element concentrations (Nakamura 1974), with a

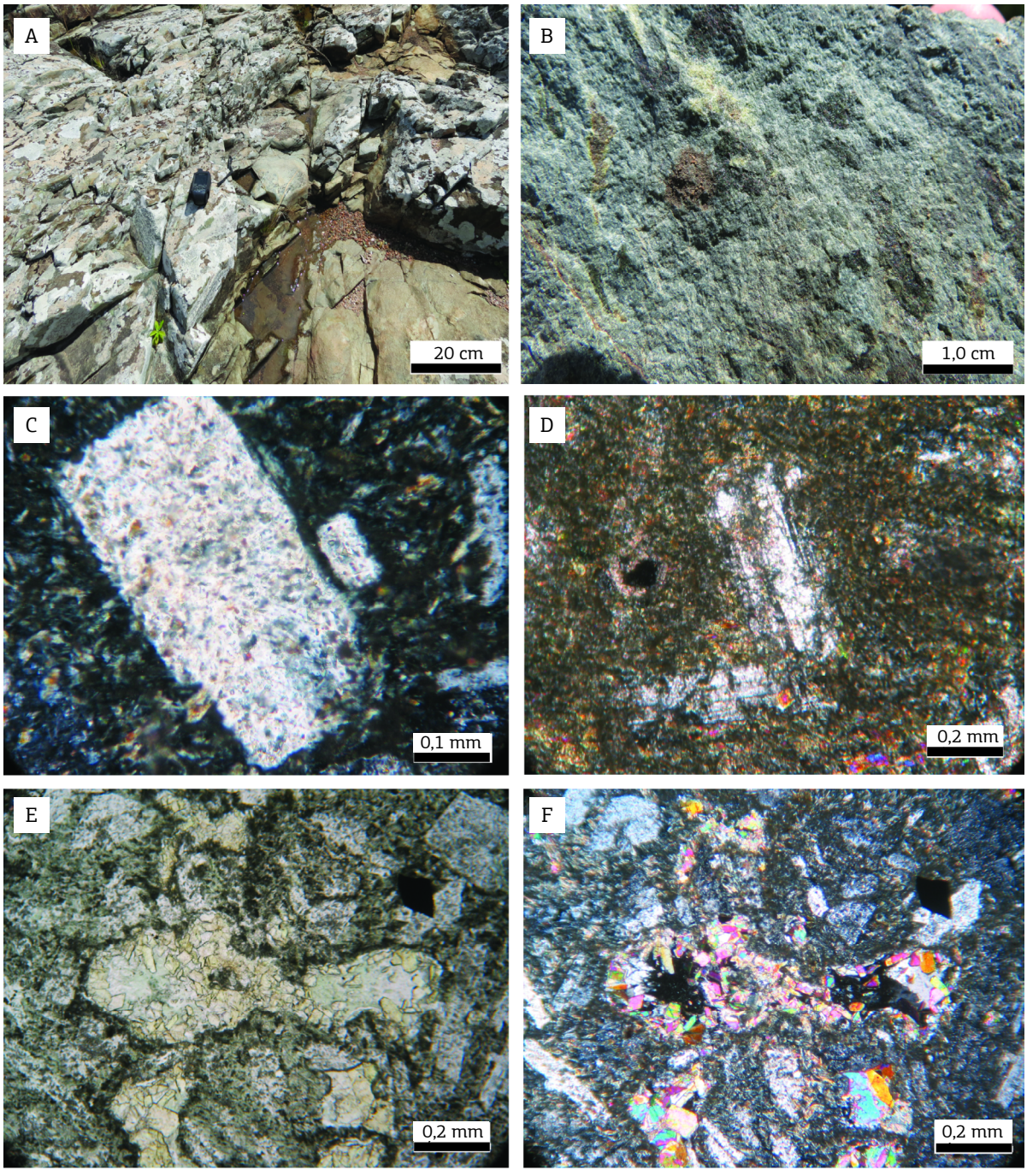

Figure 4. (A) Basalt outcrop near of the Palma stream. (B) Macroscopic aspect. (C) and (D) Photomicrographs (crossed nicols) of plagioclase phenocrysts and matrix. (E) and (F) Vesicle filled by epidote, carbonate and quartz (in "E" plane-polarized light and "F" cross-polarized light).

Table 1. Geochemical data from five of representative samples of the Acampamento Velho Formation located in Palma region.

Sample	LV-53	LV-55	LV-65	LV-70	8140A
SiO_2	53.31	53.05	51.31	49.86	57.75
Al_2O_3	18.28	17.15	17.33	13.95	15.92
Fe_2O_3	7.86	8.27	8.84	10.86	6.48
MnO	0.14	0.13	0.15	0.20	0.26
MgO	4.14	5.50	5.34	7.85	3.83
CaO	7.33	6.87	7.88	9.65	4.23
Na_2O	3.18	4.42	4.09	2.53	3.41
K_2O	1.69	0.43	0.88	1.66	1.40
TiO_2	1.00	1.05	1.17	1.13	0.58
P_2O_5	0.24	0.21	0.20	0.35	0.12
LOI	2.6	2.7	2.6	1.6	5.8
TOTAL	99.77	99.82	99.82	99.70	99.83
V	178	170	194	284	127
Rb	43.3	12.6	28.0	44.4	42.2
Sr	505.9	424.0	466.2	492.8	221.5
Y	20.6	23.1	24.5	21.2	15.7
Zr	135.5	129.1	131.7	104.9	89.6
Nb	7.0	5.1	6.0	6.3	4.2
Cs	0.6	0.2	0.8	1.1	2.0
Ba	541	232	189	1036	495
La	15.3	15.8	11.2	16.1	16.6
Ce	31.7	33.9	24.4	34.9	26.7
Pr	4.00	4.00	3.15	4.39	3.36
Nd	16.9	16.8	13.5	19.2	13.4
Sm	3.74	3.83	3.57	4.75	2.50
Eu	1.29	1.20	1.35	1.46	0.81
Gd	3.74	3.92	4.53	4.46	2.69
Tb	0.61	0.69	0.68	0.70	0.44
Dy	3.63	4.20	4.38	3.64	2.86
Ho	0.81	0.90	0.91	0.74	0.59
Er	2.20	2.61	2.51	2.19	1.71
Tm	0.36	0.33	0.40	0.36	0.25
Yb	2.34	2.43	2.52	2.13	1.59
Lu	0.32	0.35	0.39	0.31	0.24
Pb	1.7	1.7	1.0	3.8	2.0
Th	3.0	2.7	1.8	3.0	3.2
U	1.0	0.6	0.5	0.9	0.9

Weight % for major elements and ppm for trace elements.

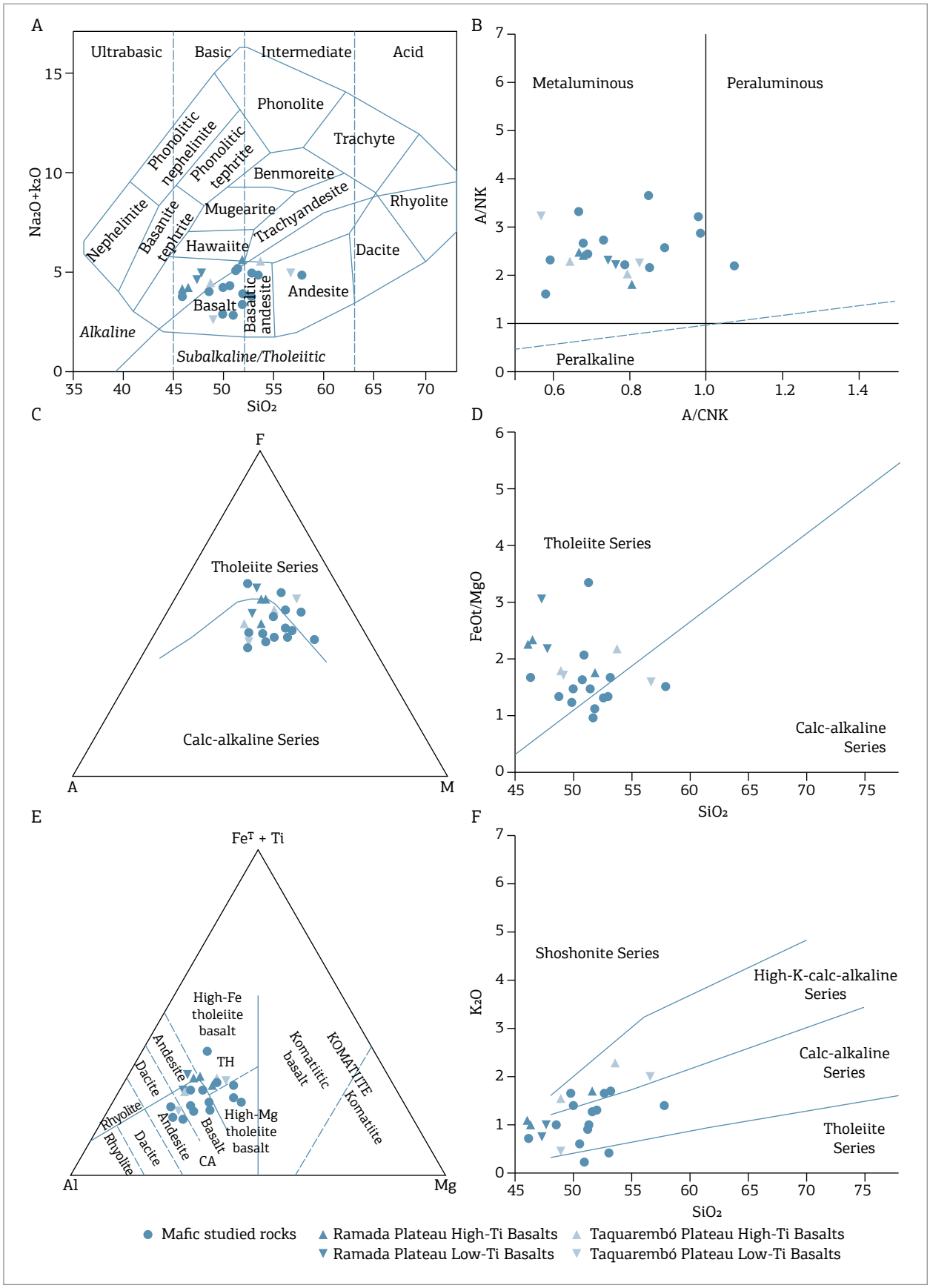

Figure 5. Chemical classifications diagrams. (A) Total Alcalis Silica (TAS) diagram (Cox *et al.* 1979). (B) Alcalis vs. alumina diagram (Shand 1943). (C) AFM (Irvine & Baragar 1971). (D) FeO/MgO vs SiO_2 (Miyashiro 1974). (E) Al-Fe+Ti-Mg diagram (Jensen 1976). (F) K2O vs SiO_2 (Le Maitre *et al.* 1989).

general enriched light rare-earth elements (LREE) pattern, incipient Eu anomalies and horizontal pattern of heavy rare earth elements (REEs) (Fig. 8A). The comparison of the ocean-island basalt (OIB)-normalized lithotypes (Sun & McDonough, 1989) shows the correlation of the basic volcanic rocks of Palma region with the low-Ti basalts of the Taquarembó and Ramada plateaus, highlighting the general higher levels of the latter. There is an enrichment in large-ion lithophile element (LILE) type elements, with a slight depletion in high field strength (HFS) elements and enrichment in heavy REE's of these lithotypes, compared to OIB (Fig. 8B).

The tectonic discrimination of the mafic volcanic rocks was investigated through the concentration of trace elements in Pearce and Cann (1973) (Fig. 9A) and Meschede (1986) (Fig. 9B) diagrams, in which the analyzed samples are concentrated mainly in the field of calc-alkaline arc basalts. The tectonic analysis by Shervais (1982) diagram shows a predominance of the Taquarembó and the Ramada plateau rocks in the context of alkaline basalts and oceanic island basalts, whereas the Palma basic rocks are in the field of retroarc basin and mid-ocean ridge basalt (MORB) basalts (Fig. 10A). In the Pearce (2008) diagrams, the Palma basalts suggest an enriched mid-ocean ridge basalts (E-MORB) source and the participation of crustal melting during the rise of magma (Fig. 10B and 10C).

Geochronology

In this study, a basalt and andesitic basalt were analyzed for U-Pb zircon geochronology. The location of the samples is indicated in Figure 3.

Andesitic basalt (sample LV-53)

The analyzed zircons show two main morphological groups:

1. Elongated and subhedral prismatic crystals, with a length/width ratio of around 1:3 and approximately 150 μm in length;
2. Equidimensional and subhedral crystals, with less than 100 μm (Fig. 11A) in length.

CL images of the analyzed crystals internally reveal concentric oscillatory zoning, characteristic of igneous rocks (Corfu *et al.* 2003). The Th/U ratios of the zircon crystals range from 0.261 to 1.286, characterizing the igneous origin (Belousova *et al.* 2002). Thirty analyses were carried out in 19 spots (Tab. 2), to obtain the $^{238}U/^{260}Pb$ and $^{235}U/^{207}Pb$ ratios, and the results of eight concordant zircons were used, whose $^{238}U/^{206}Pb$ ages ranged between 558 and 576 Ma. The selected crystals showed a $^{238}U/^{206}Pb$ and $^{207}Pb/^{206}Pb$ age of 563.3±2.1 Ma, with a mean square of weighted deviates (MSDW) of 0.0061 and concordance probability of 94% (Fig. 12).

Basalt (sample LV-70)

The LV-70 basalt zircons show elongated prismatic shape, euhedral to subhedral, with length/width ratio of around

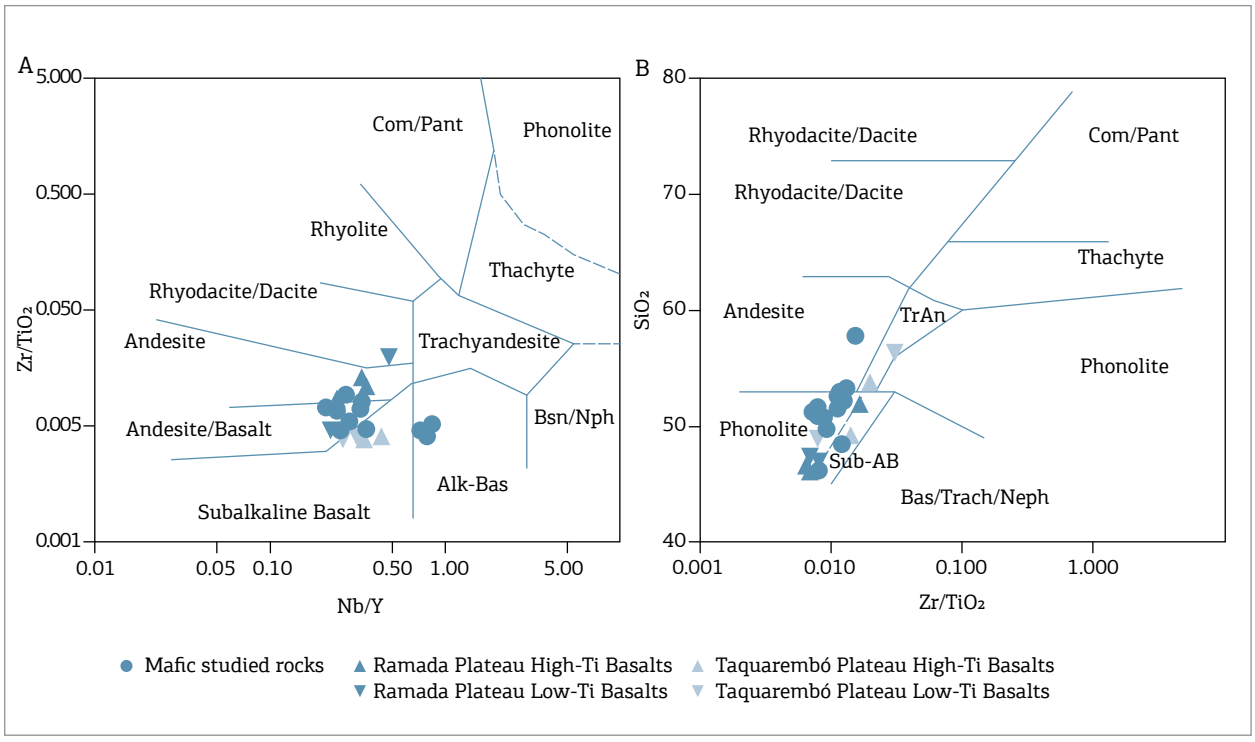

Figure 6. (A) and (B) Classification of rocks using trace elements according to Winchester and Floyd (1977) diagram.

1:3 and length between 100 and 200 μm. CL images of the zircon crystals also reveal concentric oscillatory zoning, characteristic of magmatic rocks (Corfu *et al.* 2003). This feature is confirmed by the variation of Th/U ratios of the zircon crystals, between 0.280 and 3.516. To obtain the U-Pb ages, 26 zircon crystals were analyzed, and the results of 10 concordant zircons were used (Tab. 3), whose $^{238}U/^{206}Pb$ ages ranged between 548 and 586 Ma. The selected concordant crystals showed a $^{238}U/^{206}Pb$ and $^{207}Pb/^{206}Pb$ age of 572±5.5 Ma, with MSDW of 0.052 and concordance probability of 82% (Fig. 11B). Four inherited zircon crystals were also analyzed, showing ages between 2.017 and 2.076 Ma, in which the U^{238}/Pb^{206} and Pb^{207}/Pb^{206} concordant age of 2.016±15 Ma was obtained (Fig. 13).

DISCUSSION

The Palma Complex was interpreted as an association of metamorphic rocks, generated during the orogeny that

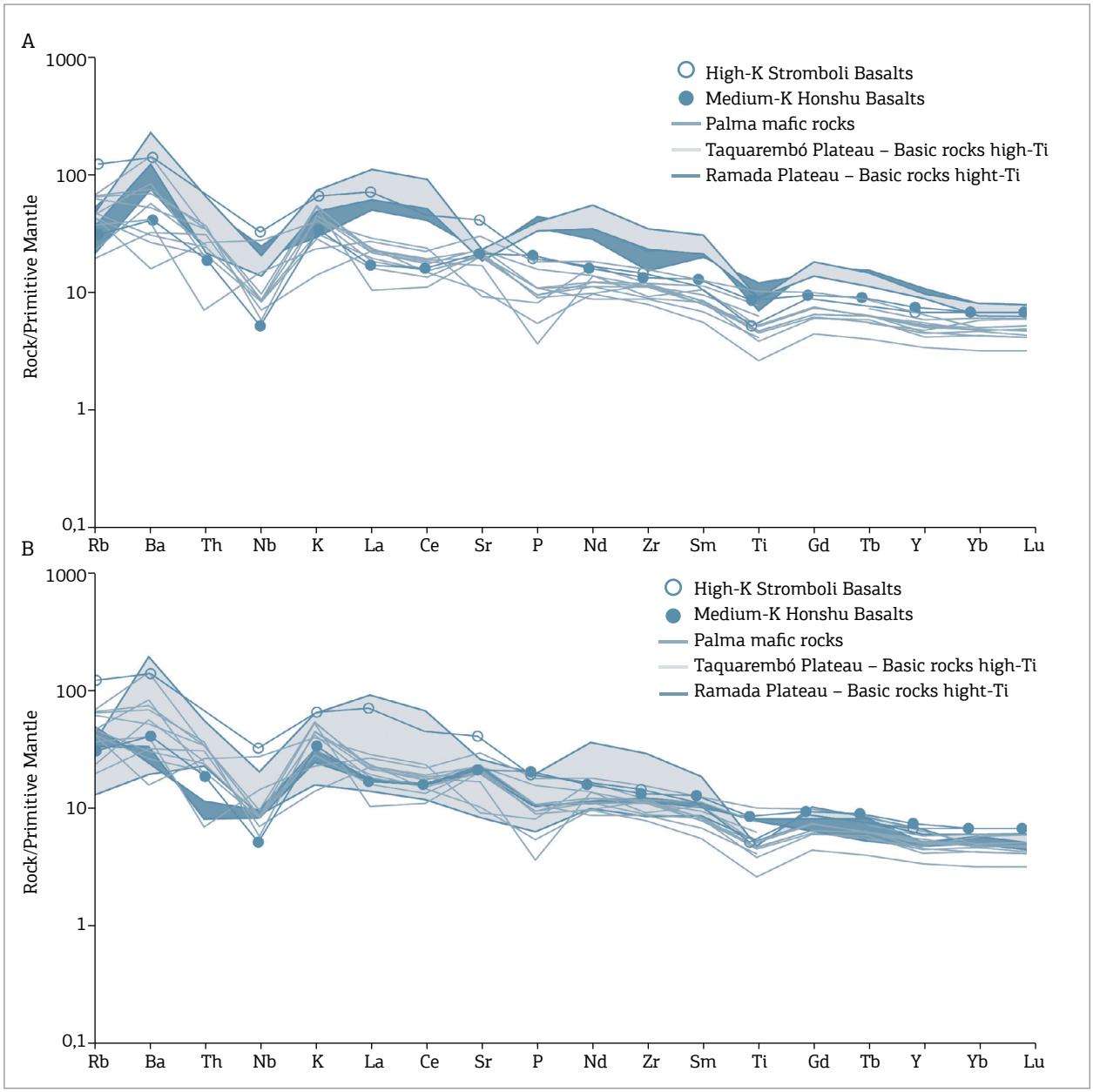

Figure 7. Multi-element diagrams (spidergrams) normalized to primitive-mantle. (A) Palma mafic rocks and High-Ti samples from Ramada (Sommer *et al.* 2005, Matté *et al.* 2016) and Taquarembó (Wildner *et al.* 2002) plateaus. (B) Palma mafic rocks and Low-Ti samples from Ramada and Taquarembó plateaus. The dates of High-K Stromboli Basalts (Francalanci *et al.* 1999) and Medium-K Honshu Basalts (Gust *et al.* 1997).

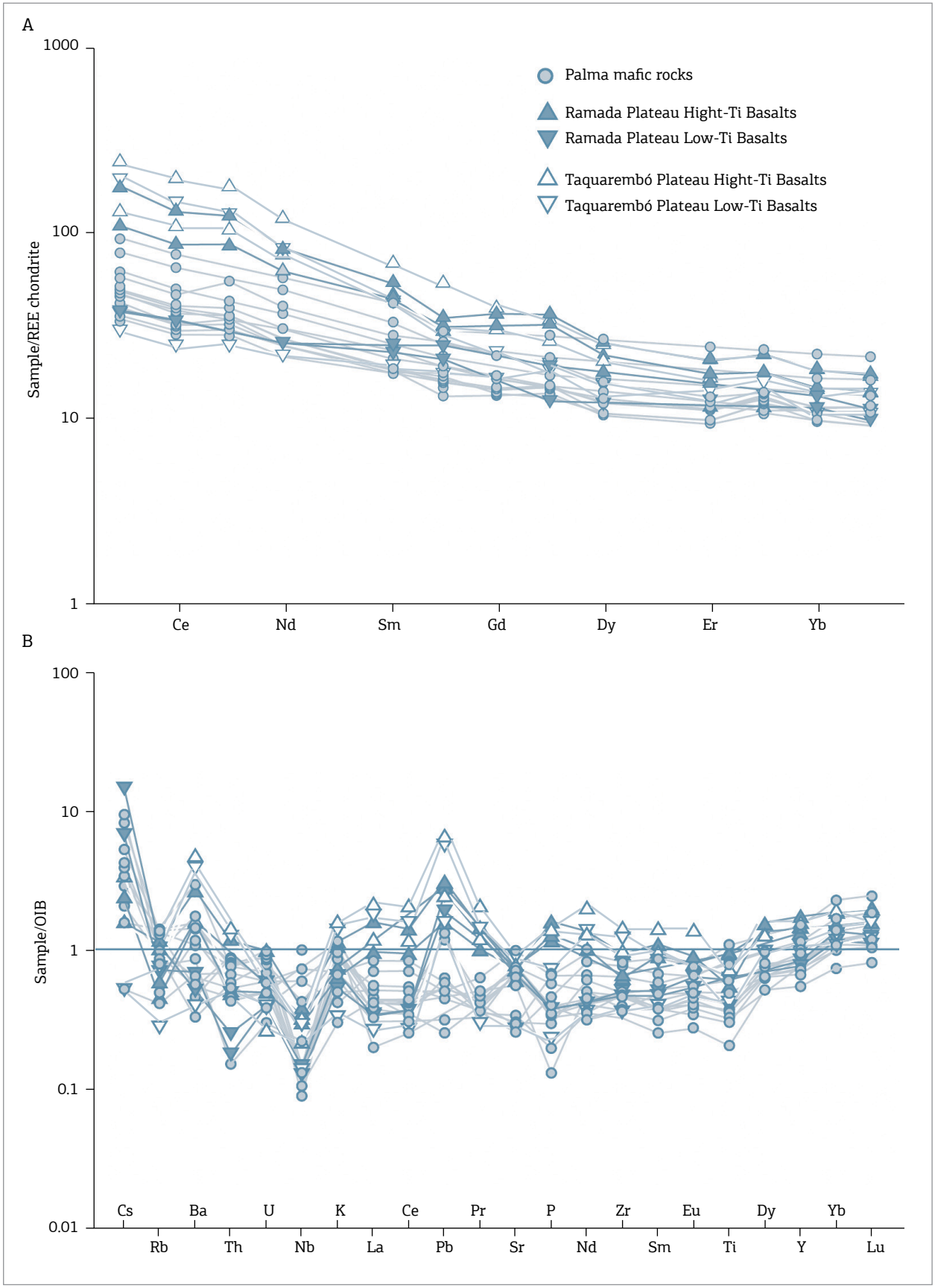

Figure 8. (A) Rare earth elements normalized to chondrite (Nakamura 1974). (B) Rare earth elements normalized to ocean-island basalt (OIB) (Sun and McDonough 1989). Dates of Taquarembó Plateau are found in Wildner *et al.* 2002 and the Ramada Plateau in Sommer et al. 2005 and Matté *et al.* 2016.

created the SGT units and part of the Dom Feliciano Belt itself (Chemale Jr. 2000, Laux *et al.* 2012). Initially, the first chemical results presented by Garcia (1980) and later by Strieder *et al.* (2000) indicated the tholeiitic character and the high levels of Al of the basalts, suggesting that they represent high aluminum basalts associated with subduction zones. This hypothesis of lithosphere subduction in an environment of active or post-collisional continental margins was reinforced by Wildner *et al.* (1999), by the presence of a comenditic trend, with Zr levels about

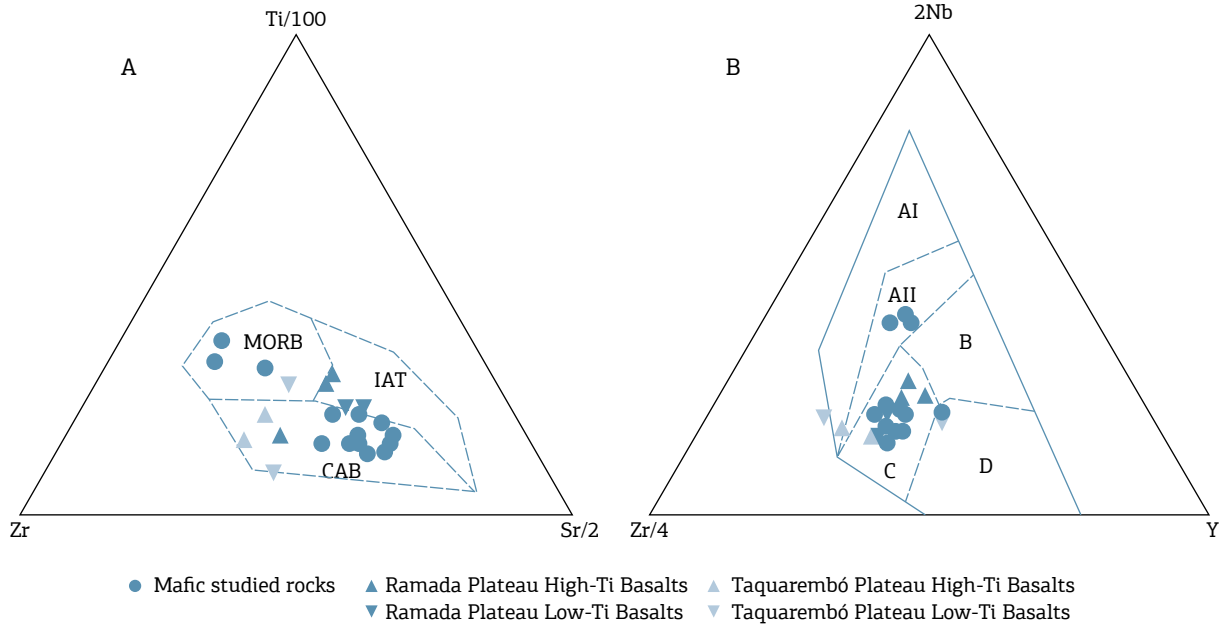

MORB: mid-ocean-ridge basalt; WPB: within-plate basalt; CAB: calc-alkaline basalt; IAT: island arc tholeiites; AI: within-plate alkali basalts; AII: Within-plate alkali and within-plate tholeiite basalts; B: plume MORB; C: Volcanic Arc Basalts and within-plate tholeiite; D: N-MORB and Volcanic Arc Basalts.

Figure 9. (A) Tectonic discrimination according to Pearce and Cann (1973) diagrams. (B) Tectonic discrimination according to Meschede (1986) diagram. Data of Taquarembó Plateau are found in Wildner *et al.* 2002 and the Ramada Plateau in Sommer *et al.* 2005 and Matté *et al.* 2016.

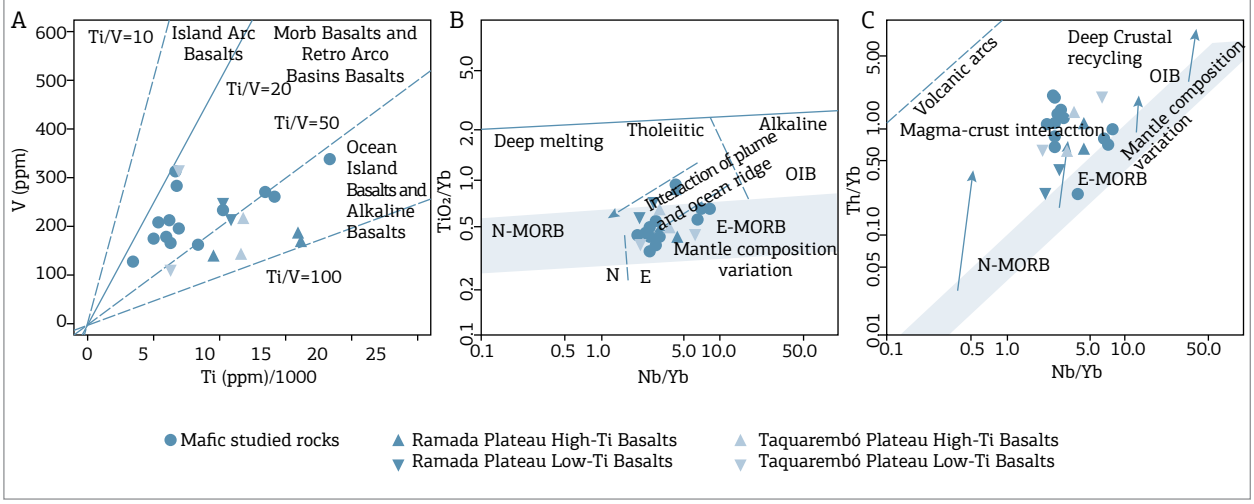

Figure 10. (A) V vs Ti diagram Shervais (1982) diagram. (B) Nb/Yb vs TiO2/Yb diagram (after Pearce 2008). (C) Th/Yb vs Nb/Yb diagram (Pearce 2008). Dates of Taquarembó Plateau are found in Wildner *et al.* 2002 and the Ramada Plateau in Sommer *et al.* 2005 and Matté *et al.* 2016.

15 times higher than the Nb levels. Subsequently, Lopes and Hartmann (2003) recognized the alkaline/tholeiitic transitional behavior of metabasalts and interpreted it as a possible oceanic plateau.

The data presented herein, however, indicate that the basic volcanic rocks previously included in the Palma Complex were not affected by orogenic metamorphism. Field and petrographic surveys carried out in the basalts show the presence of flow structures with a sub-horizontal arrangement, indicating that the body represents a sub-aerial lava flow. The elongated shape of the body, in the N45ºE direction, and the lava flow disposition suggest that the rise and positioning of the body were controlled by a tectonic structure, representing a younger reactivation stage of the Palma-Vila Nova Shear Zone (Fig. 2 and 3). The basalts exhibit porphyritic texture with high content of plagioclase phenocrysts and trachytic texture. The presence of zones rich in amygdales and vesicles indicates the preservation of the upper portion of the flow, along with intense hydrothermal alteration.

Petrographic analyses indicate that metamorphism that affected the basalts is of thermal origin and is associated with the intrusion of the Jaguari Granite. The development of actinolite porphyroblasts with radiating fiber texture and micas with decussate texture attest to the thermal metamorphism. The transformation associated with intense hydrothermal alteration gives the rocks a greenish color, which is associated with the growth of actinolite, epidote, chlorite and sericite in the basalt matrix. The low temperature metamorphism and its effects on vulcanites led the researchers to suggest that these rocks were metamorphosed. However, the decussate and radial textures and the absence of deformation features discards its transformation by orogenic metamorphism, as previously mentioned by Garcia and Hartmann (1981), Chemale Jr. (1982), Santos *et al.* (1990), UFRGS (1996), Lopes and Hartmann (2003) and Laux *et al.* (2012). The Ramada Plateau basalts have very fine-grained groundmass (40%), labradorite phenocrysts (20%) up to 1 mm, hematite (20%), and chlorite (15%) as a mafic alteration. Remnants of altered diopside are visible (5%), and apatite and rare zircon crystals represent the accessory minerals (Matté *et al.* 2016). The Taquarembó Plateau basalts have plagioclase (labradorite) in flow-oriented grains, are the dominant phase, followed by augite ranging and ilmenite microphenocrysts in a glomeroporphyritic to subophitic texture with a groundmass composed of intersertal glass, plagioclase microlites and K-feldspar (Wildner *et al.* 2002).

The basalts of the Palma region have a K/Ar age of 559±17 Ma obtained by Teixeira (1982). The U-Pb zircon analyses of basalts yielded ages of 563±2 Ma and 572±6 Ma, indicating that the rocks are Ediacaran and can be correlated with the volcanic rocks of the Acampamento Velho Formation, CB.

The CB fill was interpreted by Paim *et al.* (2000) as having occurred during the last stages of the Brasiliano Cycle orogenies. The deposition of the Maricá Group occurred in marine environment, transitioning to deep-sea conditions with associated border fans of the Bom Jardim Group. Later, the Santa Barbara Group was deposited in shallow lacustrine environment with deltas and fans, ending with the shallow lacustrine, alluvial and eolic facies of the Guaritas Group. The two first depositional cycles were controlled by transcurrent shear zones of NE-SW direction and in brittle-ductile conditions. The last depositional episodes began with the eruption of the andesites of the Hilário Formation, Bom Jardim Group, of shoshonitic affinity, going to the eruption of bimodal transitional volcanic rocks (basalts and subordinate

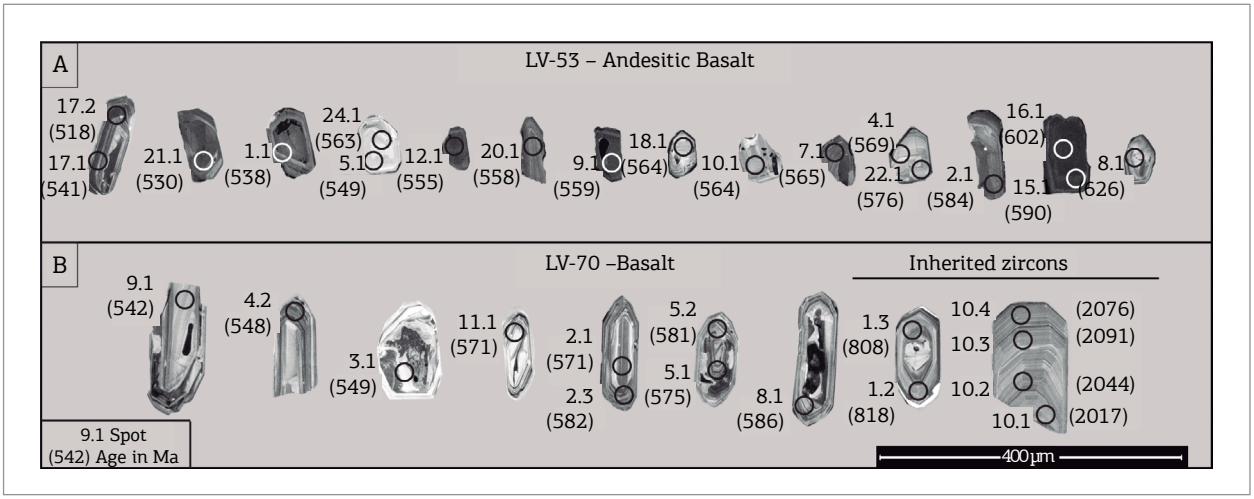

Figure 11. Cathodoluminescence image of analyzed zircons with indications of U-Pb ages in millions of years of the: (A) LV-53 sample and (B) LV-70 sample.

Table 2. LA-ICP-MS U-Pb results for igneous zircons from the sample LV-53 of the Acampamento Velho Formation.

Spot	Results											
	207/235	1 σ	206/238	1 σ	C.C	238/206	1 σ	207/206	1 σ	208/206	1 σ	*Total Pb
20.1	0.7381	0.0163	0.0904	0.0011	0.24	11.0667	0.1337	0.0592	0.0013	0.1386	0.0293	0.00
9.1	0.7351	0.0131	0.0907	0.0007	0.95	11.0295	0.0852	0.0588	0.0010	0.1270	0.0082	0.00
24.1	0.7449	0.0189	0.0913	0.0012	0.86	10.9520	0.1463	0.0592	0.0015	0.1858	0.0170	0.14
18.1	0.7458	0.0268	0.0914	0.0015	0.67	10.9384	0.1743	0.0592	0.0022	0.4052	0.0283	0.45
10.1	0.7408	0.0161	0.0915	0.0008	0.89	10.9329	0.0947	0.0587	0.0012	0.1217	0.0069	0.04
7.1	0.7447	0.0179	0.0917	0.0009	0.54	10.9071	0.1012	0.0589	0.0014	0.1022	0.0101	1.31
22.1	0.7555	0.0324	0.0935	0.0017	0.43	10.6988	0.1896	0.0586	0.0027	0.2585	0.0127	0.45
4.1	0.7579	0.0463	0.0923	0.0017	0.29	10.8353	0.1998	0.0596	0.0040	0.2041	0.0138	0.49
2.1	0.7750	0.0159	0.0948	0.0008	0.53	10.5508	0.0887	0.0593	0.0012	0.1240	0.0162	2.70
5.1	0.7244	0.0175	0.0890	0.0008	0.42	11.2404	0.1044	0.0591	0.0014	0.1520	0.0176	0.11
12.1	0.7262	0.0137	0.0899	0.0007	0.91	11.1181	0.0894	0.0586	0.0010	0.1043	0.0069	1.75
15.1	0.7749	0.0137	0.0959	0.0011	0.95	10.4319	0.1184	0.0586	0.0009	0.1165	0.0084	0.12
1.1	0.7117	0.0143	0.0870	0.0007	0.93	11.4896	0.0939	0.0593	0.0012	0.1030	0.0067	5.51
8.1	0.8377	0.0263	0.1019	0.0011	0.96	9.8099	0.1087	0.0596	0.0020	0.2153	0.0642	0.86
16.1	0.7891	0.0137	0.0979	0.0011	0.87	10.2196	0.1160	0.0585	0.0009	0.1661	0.0036	0.90
17.1	0.7159	0.0250	0.0875	0.0014	0.39	11.4325	0.1797	0.0594	0.0022	0.1889	0.0658	1.37
17.2	0.6840	0.0146	0.0837	0.0010	0.98	11.9410	0.1436	0.0592	0.0012	0.2876	0.0432	1.94
21.1	0.6983	0.0169	0.0857	0.0011	0.96	11.6638	0.1479	0.0591	0.0015	0.1119	0.0325	0.00
3.2	1.7819	0.0315	0.1721	0.0014	0.88	5.8114	0.0466	0.0751	0.0013	0.0744	0.0014	0.04

Spot	Estimated values (ppm)			Calculed ages					Conc. (%)
	Pb	Th	U	Th/U	T206/238	1 σ	T207/206	1 σ	
20.1	115.3	366.9	1172.1	0.313	0.558	0.006	0.576	0.044	96
9.1	201.4	669.9	1921.4	0.349	0.559	0.004	0.560	0.036	99
24.1	80.3	460.6	767.6	0.600	0.563	0.007	0.573	0.055	98
18.1	48.7	510.4	407.6	1.252	0.564	0.009	0.573	0.079	98
10.1	106.2	407.9	1040.7	0.392	0.564	0.005	0.557	0.046	101
7.1	68.3	201.1	696.1	0.289	0.565	0.005	0.564	0.052	100
22.1	32.9	232.5	290.7	0.800	0.576	0.010	0.553	0.096	104
4.1	19.8	118.8	181.4	0.655	0.569	0.010	0.588	0.143	96
2.1	119.5	417.1	1150.5	0.363	0.584	0.005	0.578	0.044	100
5.1	72.6	384.4	720.2	0.534	0.549	0.005	0.569	0.053	96
12.1	292.8	1322.0	2943.9	0.449	0.555	0.004	0.551	0.039	100
15.1	346.6	1167.6	3347.9	0.349	0.590	0.006	0.553	0.035	106
1.1	115.0	401.9	1221.1	0.329	0.538	0.004	0.578	0.044	93
8.1	130.5	1399.3	1087.8	1.286	0.626	0.007	0.589	0.072	106
16.1	435.3	2219.4	3974.8	0.558	0.602	0.007	0.548	0.033	109
17.1	132.6	1225.0	1087.0	1.127	0.541	0.008	0.580	0.078	93
17.2	170.0	1130.2	1665.2	0.679	0.518	0.006	0.576	0.045	90
21.1	120.8	586.2	1158.0	0.506	0.530	0.006	0.570	0.058	93
3.2	158.4	220.2	844.1	0.261	1.024	0.008	1.071	0.034	95

*Common Pb in %. CC - correlation coefficient.

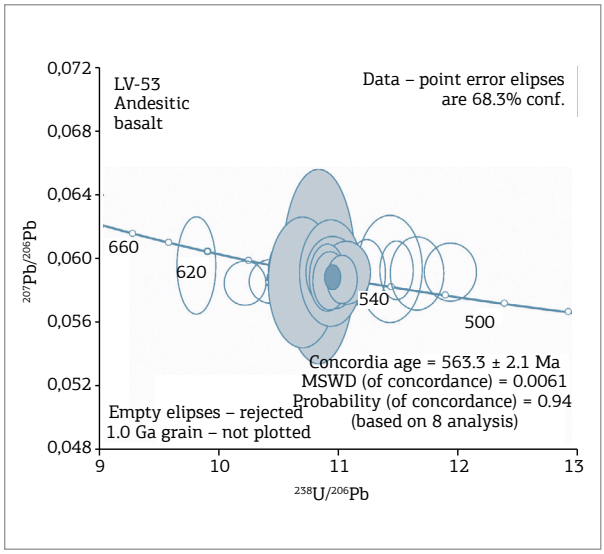

Figure 12. Concordia plot of U-Pb zircon data for the sample LV-53 of andesitic basalt from the Acampamento Velho Formation.

rhyolites), of tholeiitic to sodium alkaline nature, of the Acampamento Velho Formation, Santa Barbara Group. The volcanic activities end with the alkaline basalts of the Rodeio Velho Formation, Guaritas Group (Wildner *et al.* 2002, Almeida *et al.* 2012, Janikian *et al.* 2012). The associated granitic plutons with high-K calc-alkaline composition have U-Pb SHRIMP and LA-ICP-MS zircon ages between 598 and 570 Ma, while the alkaline plutons have crystallized between 570 and 560 Ma. Recently, Paim *et al.* (2014) proposed a review on the four evolutionary stages of the CB evolved between 630 and 510 Ma. The authors considered the CB evolution as related to the final stages of the Dom Feliciano orogeny, from tardi-orogenic basins (Maricá retroarc foreland basins and East and West Bom Jardim transcurrent basins) to post-orogenic basins (West and East Santa Barbara rifts and Guaritas Rift). Table 4 presents a review of the geochronological data of the volcanic rocks of CB.

The correlation results indicate that the basic rocks occurring in Palma village area have, however, compositional

Table 3. LA-ICP-MS U-Pb results for igneous and inherited zircons from the sample LV-70 of the Acampamento Velho Formation.

Spot	Results											
	207/235	1 σ	206/238	1 σ	C.C	238/206	1 σ	207/206	1 σ	208/206	1 σ	*Total Pb
9.1	0.6968	0.0454	0.0876	0.0025	0.73	11.4095	0.3263	0.0577	0.0037	0.1297	0.0333	0.34
11.1	0.7635	0.0322	0.0926	0.0023	0.85	10.8022	0.2663	0.0598	0.0021	0.2276	0.0244	3.46
2.1	0.7403	0.0335	0.0927	0.0012	0.34	10.7893	0.1436	0.0579	0.0026	0.3822	0.0488	0.90
5.1	0.7664	0.0196	0.0932	0.0009	0.96	10.7254	0.1018	0.0596	0.0014	0.3934	0.0610	1.79
5.2	0.7656	0.0225	0.0942	0.0010	0.91	10.6123	0.1131	0.0589	0.0016	0.1988	0.0176	1.00
2.3	0.7815	0.0325	0.0945	0.0023	0.73	10.5782	0.2600	0.0600	0.0021	0.2738	0.0425	3.05
8.1	0.7801	0.0310	0.0952	0.0022	0.98	10.5017	0.2411	0.0594	0.0022	0.1911	0.0202	4.43
3.1	0.7205	0.0299	0.0889	0.0012	0.31	11.2500	0.1471	0.0588	0.0023	1.0277	0.4188	0.00
10.1	6.1754	0.1989	0.3673	0.0087	0.94	2.7227	0.0644	0.1219	0.0029	0.2054	0.0027	0.09
10.2	6.2524	0.1984	0.3732	0.0087	0.98	2.6797	0.0626	0.1215	0.0029	0.2158	0.0037	0.12
10.3	6.2633	0.1996	0.3704	0.0087	0.84	2.6996	0.0635	0.1226	0.0029	0.2093	0.0036	0.13
10.4	6.4041	0.1959	0.3800	0.0086	0.93	2.6313	0.0599	0.1222	0.0028	0.1858	0.0029	0.08
4.2	0.7251	0.0186	0.0887	0.0009	0.97	11.2755	0.1087	0.0593	0.0014	0.2450	0.0169	1.05
1.3	1.2232	0.0355	0.1336	0.0014	0.20	7.4854	0.0802	0.0664	0.0018	0.1051	0.0080	0.22
1.2	1.2199	0.0330	0.1352	0.0014	0.59	7.3939	0.0747	0.0654	0.0016	0.1332	0.0046	0.17

Continue...

Table 3. Continuation.

Spot	Estimated values (ppm)			Calculed ages					Conc. (%)
	Pb	Th	U	Th/U	T206/238	1 σ	T207/206	1 σ	
9.1	23.0	82.2	228.3	0.360	0.542	0.015	0.517	0.138	104
11.1	53.6	362.0	449.4	0.806	0.571	0.013	0.597	0.077	95
2.1	65.8	787.5	487.7	1.615	0.571	0.007	0.527	0.092	108
5.1	103.6	876.4	906.9	0.966	0.575	0.005	0.590	0.051	97
5.2	92.8	600.5	874.0	0.687	0.581	0.006	0.564	0.058	102
2.3	68.1	657.3	571.7	1.150	0.582	0.014	0.602	0.078	96
8.1	68.2	567.4	788.5	0.720	0.586	0.013	0.582	0.080	100
3.1	14.8	350.8	99.8	3.516	0.549	0.007	0.559	0.080	98
10.1	125.7	205.9	276.1	0.746	2.017	0.041	1.985	0.043	101
10.2	130.2	222.0	288.2	0.770	2.044	0.041	1.979	0.042	103
10.3	141.8	238.1	313.6	0.759	2.031	0.041	1.995	0.043	101
10.4	174.1	259.8	384.7	0.675	2.076	0.040	1.989	0.040	104
4.2	114.7	826.3	1080.7	0.765	0.548	0.005	0.578	0.051	94
1.3	57.8	141.0	399.7	0.353	0.808	0.008	0.819	0.058	98
1.2	63.7	175.9	425.5	0.413	0.818	0.008	0.788	0.052	103

*Common Pb in %. CC - correlation coefficient

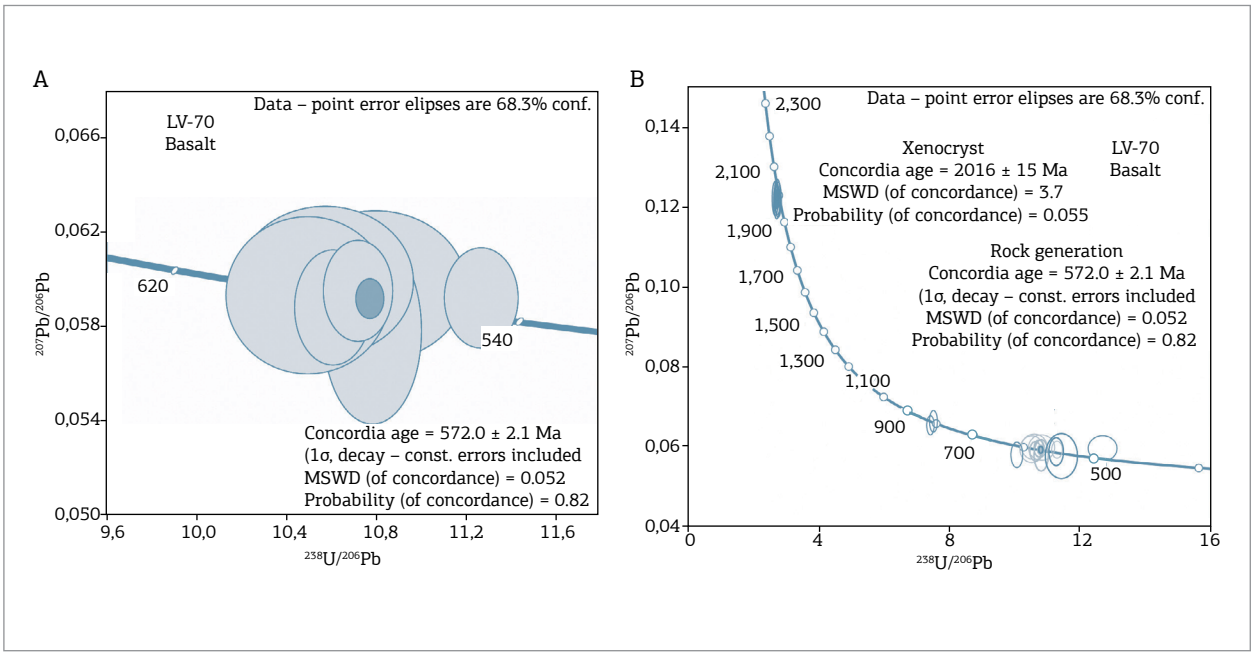

Figure 13. (A) Concordia plot of U-Pb zircon data for the sample LV-70 of basalt from the Acampamento Velho Formation. (B) Concordia of U-Pb zircon data for the sample LV-70 with inherited xenocrystals.

Table 4. Geochronological data of the volcanic rocks of Camaquã Basin.

Location	Lithoestratiphic unit	Rock type	Age	Dated mineral	Method	Source
São Gabriel Terrane						
Lavras do Sul	Lavras do Sul Granite	Granodiorite	580±7 Ma	Zircon	U-Pb SHRIMP	Remus *et al.* 1997
São Gabriel - Palma	Jaguari Granite	Syenogranite	568±7 Ma		U/Pb LA-ICP-MS	Gastal *et al.* 2010
Vila Nova do Sul	Cerro da Cria Granite	Syenogranite	564±4 Ma	Bulk Rock	Rb-Sr	Naime & Nardi 1991
FIDA Mine	Caçapava do Sul Granite	Granodiorite	562±8 Ma	Zircon	U-Pb SHRIMP	Remus *et al.* 2000
Caçapava do Sul BR-392	Caçapava do Sul Granite	Granodiorite	541±11 Ma		U-Pb SHRIMP	Leite 1998
Pedreira ao sul de São Sepé	São Sepé Granite	Monzogranite	559±7 Ma			Remus *et al.* 1997
		Syenogranite	539±7 Ma		U-Pb LA-ICP-MS	Gastal *et al.* 2010
Vila Nova do Sul	Ramada Granite		464±13 Ma	Bulk Rock	Rb/Sr	Naime & Nardi 1991
Pelotas Batholith						
Porto Alegre	Santana Granite	Perthite Granite	600±10 Ma	Zircon	U-Pb LA-ICP-MS	Koester *et al.* 2001
Canguçu	Arroio Moinho Granite	Syenogranite	595±1 Ma		U-Pb TIMS	Babinsky *et al.* 1996
Butiá	Ana Dias Rhyolite	Rhyolite	581±1.9 Ma		U-Pb LA-ICP-MS	Oliveira *et al.* 2014
Piratini	Rhyolite	Rhyolite	551±7 Ma			Zanon *et al.* 2010
Bom Jardim Group						
Casa de Pedra Region (SBC-C)	Cerro da Angélica Formation	Granitic intrusion	594±3 Ma	Zircon	U-Pb TIMS	Janikian 2004
Lavras do Sul (SBC-Oc)	Hilário Formation	Andesito	590±6 Ma	Plagioclase (andesite)	Ar-Ar	
BR-153 (SBC-C)		Lapilli tuff	589±5 Ma	Zircon	U-Pb TIMS	
			590±6 Ma			
Passo do Hilário (SBC-Oc)		Andesite	588±7 Ma	Plagioclase (andesite)	Ar-Ar	
Lavras do Sul (SBC-Oc)			586±8 Ma			
Casa de Pedra (SBC-C)	Cerro da Angélica Formation	Basic intrusion	555±22 Ma	Zircon	U-Pb TIMS	
Fazenda Fomento (SBC-C)	Picada das Graças Formation	Subvolcanic andesite	550±21 Ma			
Bom Jardim (SBC-C)	Fm. Hilário	Rhyolite	547±9 Ma			
Lavras do Sul		Andesite	512±20 Ma	Bulk Rock	K-Ar	Ribeiro & Teixeira 1970
?		Volcanic rock	510–535 Ma		Rb/Sr	Cordani *et al.*1974
Sub-Basin Camaquã Ocidental		Andesite	510±40 Ma		K-Ar	Cordani (*apud* Ribeiro & Teixeira 1970)
Lavras do Sul SBC-Oc			495±20 Ma 511±20 Ma			Minioli & Kawashita 1971
			523±20 Ma	K-Ar		
			528±20 Ma			

Continue...

Table 4. Continuation.

Location	Lithoestratiphic unit	Rock type	Age	Dated mineral	Method	Source
Acampamento Velho Formation						
Western Camaquã Sub-basin	Acampamento Velho Formation	Rhyolite pebble	580±13 Ma	Zircon	U-Pb SHRIMP	Janikian *et al.* 2012
			570±5 Ma			
Central Camaquã sub-basin		Hypabissal rhyolite	572±6 Ma		U-Pb TIMS	
E - Ramada Plateau SBC-Oc		Rhyolite	574±7 Ma			Janikian 2004
Sub-Basin Camaquã Ocidental			573±18 Ma			Chemale Jr. 2000
Ramada Plateau		Welded tuff	560±2 Ma		U-Pb ICP-MS-LA	Matté *et al.* 2016
		Traquite	560±14 Ma			
		Rhyolite	562±2 Ma			
São Gabriel - Palma		Basalt	559±17 Ma	Bulk Rock	K-Ar	Teixeira *et al.* 1982
Ramada Plateau		Rhyolite	549±5 Ma	Zircon	U-Pb SHRIMP	Sommer *et al.* 2005
Ramada Plateau/ Ramada Granite		Rhyolite	525±3 Ma			Cordani *et al.* 1974
Platô da Ramada		Ignimbrite	504±20 Ma 533±20 Ma	Bulk Rock	K-Ar RT	Minioli & Kawashita 1971
Guaritas Group						
Pedra da Arara-Cerro do Diogo	Rodeio Velho Member	Basalt	547±6.3 Ma	Zircon	U-Pb ICP-MS-LA	Almeida *et al.* 2009
?	Guaritas Formation	?	525 Ma	Clay Illite	K-Ar	Bonhome & Ribeiro 1983
Sul-Leste de Caçapava do Sul	Pedra da Pintada Formation	Alluvial facies	522±10 Ma			Maraschin *et al.* 2010
?	Rodeio Velho Member	Andesite	470±19 Ma	Zircon	U-Pb SHRIMP	Hartmann *et al.*, 1999

characteristics different from the effusive and high and low-Ti hypabyssal deposits of Acampamento Velho Formation found in the Ramada and the Taquarembó plateaus. The geochemical compositions show differences, such as the alkaline character of the basalts of the Ramada and Taquarembó plateaus and the subalkaline character of the Palma basalts. The apparent alkalinity of some samples of Palma basalts can be associated with the transformation imposed by thermal metamorphism, characterized by intense sericitization of the plagioclase phenocrysts and the matrix of the basalts. Similarly, these basalts are arranged on the boundary between the calc-alkaline and tholeiitic rock fields, and can also reflect the intense oxidation of the mafic minerals present in the matrix of vulcanites.

The high and low-Ti compositional differences of basic magmas of the Taquarembó and Ramada plateaus can be related to different melt fractions of the asthenosphere or the lithospheric mantle (Baker *et al.* 1977), derived from an intraplate rift environment or the mantle wedge affected by a subduction event (Wilson 1989). The geochemical similarity of the Palma basalts with the active subduction environment basalts may suggest that the melting conditions that generated the latter were different from the alkaline basalts of the Taquarembó and Ramada plateaus. The basalts of the plateaus show transitional characteristics between volcanic arc basalts and intraplate basalts, a typical behavior of the basalts of moderate alkaline affinity, usually related to extensional environments of continental rifts or associated with the post-collisional period of orogenic systems (Leat *et al.* 1986).

The basalts of the Palma area have compositions similar to calc-alkaline arc basalts. These characteristics may be associated with the source rocks that constitute the SGT. The units of this terrane were generated by subduction processes and present geochemical composition of juvenile rocks. In the same way, the underlying mantle presents the

effects of metassomatism associated with the fluids involved during the subduction processes.

The generation of this magmatism is associated with the post-collisional evolution period of the Dom Feliciano Belt.

CONCLUSIONS

Data integration shows that the basalts of the Palma village area belong to the Acampamento Velho Formation, of the Santa Barbara Group and CB.

The calc-alkaline characteristics of this magmatism differ with respect to the basic volcanic rocks occurring in the Ramada and Taquarembó plateaus, which have alkaline character. Geochemical data suggest that the basic volcanic rocks studied were generated from the partial melting of a lithospheric mantle affected by previous subduction events.

ACKNOWLEDGEMENTS

We would like to acknowledge the Brazilian National Council for Scientific and Technological Development (CNPq) for the research grants, the Geoscience Institute of Universidade Federal do Rio Grande do Sul State (UFRGS) for field work support and laboratories, and the Geochronology Research Center of Universidade de São Paulo (USP), for the access to LA-ICP-MS laboratory. We are grateful to Jorge Laux, Miguel A.S. Basei and reviewers for the helpful comments and suggestions.

REFERENCES

Almeida D.P.M., Chemale Jr. F., Machado A. 2012. Late to Post-Orogenic Brasiliano-Pan-African Volcano-Sedimentary Basins in the Dom Feliciano Belt, Southernmost Brazil. *Petrology – New Perspectives and Applications*, pp. 73-135.

Almeida D.P.M., Zerfass H., Basei M.A., Petry K., Gomes C.H. 2002. The Acampamento Velho Formation, a Lower Cambrian bimodal volcanic package: Geochemical and stratigraphic studies from the Cerro do Bugio, Perau and Serra de Santa Bárbara (Caçapava do Sul, Rio Grande do Sul, RS–Brazil). *Gondwana Research,* **5**(3):721-733.

Almeida R.P., Janikian L., Fragoso-Cesar A.R.S, Fambrini G.L. 2010. The Ediacaran to Cambrian Rift System of Southeastern South America: Tectonic Implications. *The Journal of Geology*, **118**(2):145-161.

Almeida R.P., Janikian L., Fragoso-Cesar A.R.S., Marconato A. 2009. Evolution of a rift basin dominated by subaerial deposits: The Guaritas Rift, Early Cambrian, Southern Brazil. *Sedimentary Geology*, **217**(1-4):30-51.

Babinski M., Chemale Jr. F., Hartmann L.A., Van Schmus W.R., Silva L.C. 1996. Juvenile accretion at 750-700 Ma in Southern Brazil. *Geology*, **24**(5):439-442.

Baker B.H., Goles G.G., Leeman W.P., Lindstrom M.M. 1977. Geochemistry and petrogenesis of a basalt-benmoreite-trachyte suite from the Southern part of the Gregory Rift, Kenya. *Contributions to Mineralogy and Petrology*, **64**(3):303-332.

Belousova E., Griffin W., O'Reilly S.Y., Fisher N. 2002. Igneous zircon: trace element composition as an indicator of source rock type. *Contributions to Mineralogy and Petrology,* **143**(5):602-622.

Bicca M.M., Chemale Jr. F., Jelinek A.R., Oliveira C.H.E., Guadagnin F., Armstrong R. 2013. Tectonic evolution and provenance of the Santa Bárbara Group, Camaquã Mines region, Rio Grande do Sul, Brazil. *Journal of South American Earth Sciences*, **48**:173-192.

Bonhome M.E., Ribeiro M.J., 1983. Datações K/Ar das argilas associadas à mineralização de cobre da Mina Camaquã e suas encaixantes. *In:* I Simpósio Sul-Brasileiro de Geologia. Sociedade Brasileira de Geologia. *Atas*... p. 82-88.

Borba A.W., Mizusaki A.M.P., Santos J.O.S., McNaughton N.J., Onoe A.T., Hartmann L.A. 2008. U-Pb zircon and ^{40}Ar-^{39}Ar K-feldspar dating of syn-sedimentary volcanism of the Neoproterozoic Maricá Formation: Constraining the age of foreland basin inception and inversion in the Camaquã Basin of southern Brazil. *Basin Research*, **20**(3):359-375.

Chemale Jr. F. 1982. *Geologia da Região de Palma, São Gabriel, Rio Grande do Sul*. Dissertation, Instituto de Geociências, Universidade Federal do Rio Grande do Sul, Porto Alegre, 136 p.

Chemale Jr. F. 2000. Evolução Geológica do Escudo Sul-Riograndense. *In*: Holz M., De Ros L.F. (eds.) *Geologia do Rio Grande do Sul*. Centro de Investigação do Gondwana, Instituto de Geociências, Universidade Federal do Rio Grande do Sul, Porto Alegre, p. 13-52.

Chemale Jr. F., Babinski M. 1995. U-Pb zircon dating of deformational events from the Neoproterozoic rocks in the Eastern Brazil. *In*: V Simpósio Nacional de Estudos Tectônicos. Gramado: Rio Grande do Sul, Brasil, *Boletim de Resumos Expandidos, Anais...*, p. 377-378.

Chemale Jr. F., Kawashita K., Dussin I.A., Ávila J.N., Justino D., Bertotti A. 2012. U-Pb zircon in situ dating with LA-MC-ICP-MS using a mixed detector configuration. *Anais da Academia Brasileira de Ciências*, **84**(2):275-296.

Cordani U.G., Halpern M., Berenholc M. 1974. Comentários sobre as determinações geocronológicas da Folha de Porto Alegre. *In*: Carta Geológica do Brasil ao Milionésimo. *Texto explicativo das folhas de Porto Alegre e Lagoa Mirim*, DNPM, Brasília, p. 70-77.

Corfu F., Hanchar J.M., Hoskin P.W.O., Kinny P. 2003. Atlas of zircon textures. *Reviews in Mineralogy and Geochemistry*, **53**(1):469-500.

Cox K.G., Bell J.D., Pankhurst R.J. 1979. *The Interpretation of Igneous Rocks*. London, George Allen & Unwin, 450 p.

Elhlou S., Belousova E., Griffin W.L., Peasom N.J., O'Reilly S.Y. 2006. Trace element and isotopic composition of GJ red zircon standard by laser ablation. *Geochimica and Cosmochimica Acta*, **70**(18):158.

Fernandes L.A., Tommasi A., Porcher C.C. 1992. Deformation patterns in the southern Brazilian branch of the Dom Feliciano Belt: A reappraisal. *Journal of South American Earth Sciences*, **5**(1):77-96.

Francalanci L., Tommasini S., Conticelli S., Davies G.R. 1999. Sr isotope evidence for short magma residence time for the 20th century activity at Stromboli volcano, Italy. *Earth and Planetary Science Letters*, **167**(1-2):61-69.

Garcia M.A.M. 1980. *Petrologia do Complexo Palma, Rio Grande do Sul*. Dissertation, Instituto de Geociências, Universidade Federal do Rio Grande do Sul, Porto Alegre, 133 p.

Garcia M.A.M., Hartmann L.A. 1981. Petrologia do Complexo Palma-RS. *Acta Geológica Leopoldensia*, **5**(13):51-122.

Gastal M.C., Lafon J.M., Chemale Jr. F. 2010. U-Pb and Pb-Pb zircon ages of Neoproterozoic-Eopaleozoic granites from the western portion of the southerm Brazilian Shield. *In*: VII South American Symposium on Isotopic Geology. Brasília, *Short Papers*, p.105-108.

Gõni J.C., Goso H., Issler R.S. 1962. Estratigrafia e geologia econômica do pré-cambriano e eopaleozóico uruguaio e sul-riograndense. Porto Alegre. *Avulso da Escola de Geologia*, **3**:1-105.

Gubert M.L., Philipp R.P., Basei M.A.S. 2016. The Bossoroca Complex, São Gabriel Terrane, Dom Feliciano Belt, southernmost Brazil: U-Pb geochronology and tectonic implications for the Neoproterozoic São Gabriel Arc. *Journal of South American Earth Sciences*, **70**:1-17.

Gust D.A., Arculus R.J., Kersting A.B. 1997. Aspects of magma sources and processes in the Honshu Arc. *The Canadian Mineralogist*, **35**(2):347-365.

Hartmann L.A., Chemale Jr. F., Philipp R.P. 2007. Evolução Geotectônica do Rio Grande do Sul no Pré-Cambriano. *In*: Frantz J.C., Iannuzzi R. (eds.) *50 anos de Geologia no Rio Grande do Sul*. 1° ed. Instituto de Geociências, Porto Alegre, RS: Editora Comunicação e Identidade, CIGO/UFRGS, **1**:97-123.

HartmannL.A., Nardi L.V.S., Formoso M.L.L., Remus M.V.D., Lima E.F., Mexias A. 1999. Magmatism and metallogeny in the crustal evolution of Rio Grande do Sul shield, Brazil. *Pesquisas em Geociências (UFRGS)*, **26**(2):45-63.

Hartmann L.A., Philipp R.P., Santos J.O.S., McNaughton N.J. 2011. Time frame of 753-680 Ma juvenile accretion during the São Gabriel orogeny, southern Brazil. *Gondwana Research*, **19**:84-99.

Hartmann L.A., Santos J.O.S., McNaughton N.J. 2008. Detrital zircon U-Pb age data, and Precambrian provenance of the Paleozoic Guaritas Formation, southern Brazilian Shield. *International Geology Review*, **50**(4):364-374.

Irvine T.N., Baragar W.R.A. 1971. A guide to the chemical classification of the common volcanic rocks. *Canadian Journal of Earth Sciences*, **8**(5):523-548.

Jackson S.E., Pearson N.J., Griffin W.L., Belousova E.A. 2004. The application of laser ablation-inductively coupled plasma-mass spectrometry to in situ U–Pb zircon geochronology. *Chemical Geology*, **211**(1-2):47-69.

Janikian L. 2004. *Seqüências deposicionais e evolução paleoambiental do Grupo Bom Jardim e da Formação Acampamento Velho, Supergrupo Camaquã, Rio Grande do Sul*. PhD Thesis, Instituto de Geociências, Universidade de São Paulo, São Paulo, 189 p.

Janikian L., Almeida R.P., Fragoso-Cesar A.R.S., Martins V.T.S., Dantas E.L., Tohver E., McReath I., D'Agrella-Filho M.S. 2012. Ages (U-Pb SHRIMP and LA ICPMS) and stratigraphic evolution of the Neoproterozoic volcano-sedimentary successions from the extensional Camaquã Basin, Southern Brazil. *Gondwana Research*, **21**(2-3):466-482.

Jensen L.S. 1976. *A new cation plot for classifying subalkaline volcanic rocks*. Ontario Division of Mines, Miscellaneous, 66 p.

Koester E., Soliani Jr. E., Leite J.A.D., Hartmann L.A., Fernandes L.A.D., McNaughton N.J., Santos J.O.S., Oliveira L.D. 2001. SHRIMP U-Pb age for the emplacement of Santana granite and reactivation of the Porto Alegre Suture, southern Brazil. *Journal of South American Earth Sciences*, **14**(1):91-99.

Laux J.H., Bongiolo E.M., Klein C., Iglesias C.M.F. 2012. *Mapa Geológico Lagoa da Meia Lua SH-21-Z-B-VI, escala 1:100.000*. Porto Alegre, CPRM – Serviço Geológico do Brasil, v. 1.

Leat P.T., Jackson S.E., Thorpe R.S., Stillman C.J. 1986. Geochemistry of bimodal basalt-subalkaline/peralkaline rhyolite provinces within the Southern British Caledonides. *Journal of Geological Society*, **143**(2):259-273.

Leite J.A.D., Hartmann L.A., McNaughton N.J., Chemale Jr. F. 1998. SHRIMP U/Pb zircon geochronology of Neoproterozoic juvenile and crustal-reworked terranes in southernmost Brazil. *International Geology Review*, **40**(8):688-705.

Le Maitre R.W., Bateman P., Dudek A., Keller J., Lameyre J., Le Bas M.J., Sabine P.A., Schmid R., Sörensen H., Streckeisen A., Wooleen A.R., Zanettin B. 1989. *A Classification of lgneos Rocks and Glossary of Terms: Recommendations of the International Union of Geological Sciences Subcommission on the Systematics of Igneous Rocks*. Blackwell Scientific Publications, Oxford.

Lena L.O.F., Pimentel M., Philipp R.P., Armstrong R., Sato K. 2014, The evolution of the Neoproterozoic São Gabriel Juvenile terrane, southern Brazil based on high spatial resolution U-Pb ages and ^{18}O data from detritals zircons. *Precambrian Research*, **247**:126-138.

LopesA.P., Hartmann L.A. 2003. Geoquímica de rochas metabasálticas da mina da Palma, Bloco São Gabriel, escudo sul-rio-grandense: um possível platô oceânico. *Pesquisas em Geociências*, **30**(1):27-39.

Ludwig K.R. 2008. *Manual for Isoplot 3.7*. Berkeley Geochronology Center, Special Publication No. 4, 77 p.

Maraschin A.J., Mizusaki A.M., Zwingmann H., Borba A.W., Sbrissa G.F., 2010.

Illite authigenesis in sandstones of the Guaritas Allogroup (Early Paleozoic):

Implications for the depositional age, stratigraphy and evolution of the Camaquã

Basin (Southern Brazil). *Journal of South American Earth Sciences*, **29**(2):400-411.

Matté V., Sommer C.A., Lima E.F., Philipp R.P., Basei M.A.S. 2016. Post-collisional Ediacaran volcanism in oriental Ramada Plateau, southern Brazil. *Journal of South American Earth Sciences*, **71**:201-222.

Meschede M. 1986. A method of discriminating between different types of Mid-Ocean Ridge Basalts and continental tholeiites with the Nb-Zr-Y diagram. *Chemical Geology*, **56**:207–218.

Minioli B., Kawashita K. 1971. Contribuição à estratigrafia do Eo-paleozóico do Escudo Sulrio-grandense. *In*: 25° Congresso Brasileiro de Geologia. São Paulo, *Anais...*, p. 193-198.

Miyashiro A. 1974. Volcanic rock series in island arcs and active continental margins. *American Journal of Science*, **274**(4):321-355.

Naime R.H., Nardi L.V.S. 1991. O Granito da Ramada, porção oeste do Escudo Sul-riograndense: geologia, petrologia e geoquímica. *Revista Brasileira de Geociências*, **21**(3):266-274.

Nakamura N. 1974. Determination of REE, Ba, Fe, Mg, Na and K in carbonaceous and ordinary chondrites. *Geochimica et Cosmochimica Acta*, **38**(5):757-775.

Oliveira C.H.E., Chemale Jr. F., Jelinek A.R., Bicca M.M., Phillip R.P. 2014. U-Pb and Lu-Hf isotopes applied to the evolution of the late to post-orogenic transtensional basins of the Dom Feliciano Belt, Brazil. *Precambrian Research*, **246**:240-255.

Paim P.S.G., Chemale Jr. F., Lopes C. 2000. A Bacia do Camaquã. *Geologia do Rio Grande do Sul*. Porto Alegre, CIGO/UFRGS, p. 231-274.

Paim P.S.G., Chemale Jr. F., Wildner W. 2014. Estágios evolutivos da Bacia do Camaquã (RS). *Ciência e Natura*, **36**:183-193.

Pearce J.A. 2008. Geochemical fingerprinting of oceanic basalts with applications to ophiolite classification and the search for Archean oceanic crust. *Lithos*, **100**(1-4):14-48.

Pearce J.A., Cann J.R. 1973. Tectonic setting of basic volcanic rocks determined using trace element analyses. *Earth Planetary Science Letters*, **19**(2):290-300.

Philipp R.P., Bitencourt M.F., Junges S.L. 2008. Isótopos de Nd dos Complexos Neoproterozóicos Cambaí e Cambaizinho, Terreno Vila Nova: implicações para a evolução do Cinturão Dom Feliciano no RS. *In*: 46° Congresso Brasileiro de Geologia. Curitiba, *Anais...*, p. 21.

Philipp R.P., Pimentel M.M., Chemale Jr. F. 2016. Tectonic evolution of the Dom Feliciano belt in Southern Brazil: geological relationships and U-Pb geochronology. *Brazilian Journal of Geology*, **46**(Suppl 1):83-104.

Remus M.V.D., Hartmann L.A., McNaughton N.J., Groves D.I., Fletcher I.R. 2000. The link between hydrothermal epigenetic copper mineralization and the Caçapava Granite of the Brasiliano Cycle in southern Brazil. *Journal of South American Earth Sciences*, **13**(3):191-216.

Ribeiro M., Bocchi P.R., Figueiredo Filho P.M., Tessari R.I. 1966. *Geologia da Quadrícula de Caçapava do Sul, Rio Grande do Sul*. Boletim 127. Rio de Janeiro, DNPM/DFPM. 232 p..

Ribeiro M., Fantinel L.M. 1978. Associações petrotectônicas do Escudo Sul- Riograndense: I Tabulação e distribuição das associações petrotectônicas do Escudo do Rio Grande do Sul. *Inheríngia, Série Geológica*, **5**:19-54.

Ribeiro M., Teixeira C.A.S. 1970. Datações de rochas do Rio Grande do Sul e sua influência nos conceitos estratigráficos e geotectônicos locais. *Inheríngia, Série Geológica*, **3**:109-120.

Robertson J.F. 1966. Revision of the stratigraphy and nomenclature of rock units in the Caçapava-Lavras region. State of Rio Grande do Sul, Brazil. *Notas e estudos* IG/UFRGS, **1**(2):41-54.

Saalmann K., Hartmann L.A., Remus M.V.D., Koester E., Conceição R.V. 2005. Sm-Nd isotope geochemistry of metamorphic volcano-sedimentary successions in the São Gabriel Block, southernmost Brazil: Evidence for the existence of juvenile Neoproterozoic oceanic crust to the east of the La Plata Craton. *Precambrian Research*, **136**:159-175.

Saalmann K., Gerdes A., Lahaye Y., Hartmann L.A., Remus M.V.D., Laufer A. 2010. Multiple accretion at the eastern margin of the Rio de la Plata craton: the prolonged Brasiliano orogeny in southernmost Brazil. *International Journal of Earth Sciences*, **100**(2-3):355-378.

Santos E.L., Azevedo G.C., Maciel L.A., Mosmann R., Remus M.V.D. 1990. Mapeamento geológico de sequências metavulcano-sedimentares do oeste do Escudo Sul-Riograndense, RS. *In*: 36° Congresso Brasileiro de Geologia. Natal, *Anais...*, v. 6, p. 2976-2990.

Shand S.J. 1943. *The Eruptive Rocks*, 2nd ed. New York, John Wiley, 444 p.

Shervais J.W. 1982. Ti-V plots and the petrogenesis of modern ophiolitic lavas. *Earth Planetary Science Letters*, **59**(1):101-118.

Sommer C.A., Lima E.F., Nardi L.V.S. 1999. Evolução do vulcanismo alcalino da porção sul do Platô do Taquarembó, Dom Pedrito, RS. *Brazilian Journal of Geology*, **29** (2):245-254.

Sommer C.A, Lima E., Nardi L.V.S., Figueiredo A.M.G., Pierosan R. 2005. Potassic and low- and high-Ti mildly alkaline volcanism in the Neoproterozoic Ramada Plateau, southermost Brazil. *Journal of South American Earth Sciences*, **18**(3):237-254.

Sommer C.A., Lima E.F., Pierosan R., Machado A. 2011. Reoignimbritos e ignimbritos de alto grau do Vulcanismo Acampamento Velho, RS: origem e temperatura de formação. *Brazilian Journal of Geology*, **41**(3):420-435.

Stacey J.S., Kramer J.D. 1975. Approximation of terrestrial lead isotope evolution by a two-stage model. *Earth and Planetary Science Letters*, **26**(2):207-221.

Strieder A.J., Roldão D.G., Hartmann L.A. 2000. The Palma Volcano-Sedimentary Supersuite, Precambrian Sul-Riograndense Shield, Brazil. *International Geology Review*, **42**(11):984-999.

Sun S.S., McDonough W.F. 1989. Chemical and isotopic systematics of oceanic basalts: Implications for mantle composition and processes. *Geological Society of London Special Publication*, **42**:313-345.

Teixeira W. 1982. *Folhas SH.22 – Porto Alegre, SI.22 – Lagoa Mirim e SH.21 – Uruguaiana*. Interpretação dos Dados Radiométricos e Evolução Geocronológica. Projeto RADAMBRASIL. *Florianópolis* (Relatório Interno, Inédito).

UFRGS. 1996. *Mapeamento Geológico 1:25.000 Projeto Lagoa da Meia Lua - Rufino Farias - Vila Nova: Geologia da Faixa X*. Monografia de Conclusão de Curso, Instituto de Geociências, Universidade Federal do Rio Grande do Sul, Porto Alegre, 178 p.

Wildner W., Lima E.F., Nardi L.V.S., Sommer C.A. 2002. Volcanic cycles and setting in the Neoproterozoic III to Ordovician Camaquã Basin succession in Southern Brazil: Characteristics of post-collisional magmatism. *Journal of Volcanology and Geothermal Research*, **118**(1-2):261-283.

Wildner W., Nardi L.V.S., Lima E.F. 1999. Post-collisional Alkaline Magmatism on the Taquarembó Plateau: A well-Preserved Neoproterozoic-Cambrian Plutono-volcanic Association in Southern Brazil. *International Geology Review*, **41**(12):1082-1098.

Wilson M. 1989. *Igneous petrogenesis, a global tectonic approach*. London, Unwin Hyman, 466 p.

Winchester J.A., Floyd P.A. 1977. Geochemical discrimination of different magma series and their differentiation products using immobile elements. *Chemical Geology*, **20:**325-343.